Anomalies of the Cerebellum

5

The cerebellum and brainstem are the major contents of the posterior cranial fossa (PCF). The PCF is anteriorly and laterally bounded by the sphenoid and petrous temporal bones, posteriorly and inferiorly by the squamous and basilar parts of the occipital bone and superiorly by the tentorium. The ultrasound visualisation of the PCF is impaired due to the osseous boundaries, especially in the late second and third trimesters. Knowledge of the embryology of the cerebellum is essential to understand the normal variants and defects that may occur in the PCF.

During 8–10 weeks of gestational age, the roof of the rhombencephalic vesicle (future fourth ventricle) is formed by the tela choroidea and is termed the area membranacea. The rostral half of this membrane gives rise to the vermis and the hemispheres of the cerebellum. The caudal half of the area membranacea simultaneously bulges out dorsally to form the Blake's pouch. The developing midline vermis grows inferiorly to progressively cover the roof of the fourth ventricle. The cerebellar hemispheres also develop at the same time. This results in the constriction of the base of the Blake's pouch to form its neck (metapore) from which the pouch extends into the cisterna magna. The metapore is therefore immediately inferior to the vermis. Ultimately, when the Blake's pouch fenestrates, the metapore forms the midline foramen of Magendie through which the fourth ventricle communicates with the cisterna magna.

The vermis completely 'covers' the roof of the fourth ventricle by 18 weeks of gestation. The normal finding of the vermis separating the fourth ventricle from the cisterna magna, in the axial transcerebellar section, is therefore seen after 18 weeks. Prior to 18 weeks, the vermis between the cerebellar hemispheres is not seen completely, and the fourth ventricle is seen to communicate with the cisterna magna. This is termed the 'open fourth ventricle' and is normal until 18 weeks. After 18 weeks, the 'open fourth ventricle' is an abnormal finding and may be due to a rotated or hypoplastic vermis (in midsagittal section). The foramen of Magendie is the major route through which CSF drains into the cisterna magna. The lateral foramina of Luschka, alone, are insufficient for the effective drainage of the fourth ventricle. If the Blake's pouch fenestration is delayed or does not occur, the CSF volume and pressure in the pouch build up. Delayed fenestration of the foramina of Luschka may contribute to enlargement of the Blake's pouch.

Vermian size and shape are assessed in the midsagittal section. Vermian size is assessed by cephalocaudal and anteroposterior dimensions. Vermian shape is said to be normal if it is kidney bean shaped with presence of the fastigium and primary fissure. In the midsagittal section, a normal (unrotated) vermis is parallel to the brainstem with the fourth ventricle in between. When the vermis is rotated, its lower pole is lifted off the brainstem. With increasing degrees of rotation, the brainstem vermis angle progressively increases.

Increasing degrees of Blake's pouch dilatation result in a spectrum of PCF conditions. In the order of severity, these are mega cisterna magna (MCM), Blake's pouch cyst (BPC), vermian hypoplasia (VH) and Dandy-Walker malformation (DWM) (Fig. 5.1).

5.1 Mega Cisterna Magna

The Blake's pouch expands to a size more than normal, increasing the size of the cisterna magna.

The ultrasound findings are as follows:

1. Cisterna magna is said to be enlarged when the anteroposterior depth is 10 mm or more (18 weeks onwards) (Figs. 5.2 and 5.3).
2. 'Open fourth ventricle' is not seen.
3. The vermis is normal in shape, size and position in the midsagittal section.
4. No vermian rotation is noted. The brainstem vermis angle is normal (9° ± 3.5°).
5. Mega cisterna magna is usually an isolated finding.

B. S. Rama Murthy, *Imaging of Fetal Brain and Spine*, https://doi.org/10.1007/978-981-13-5844-9_5

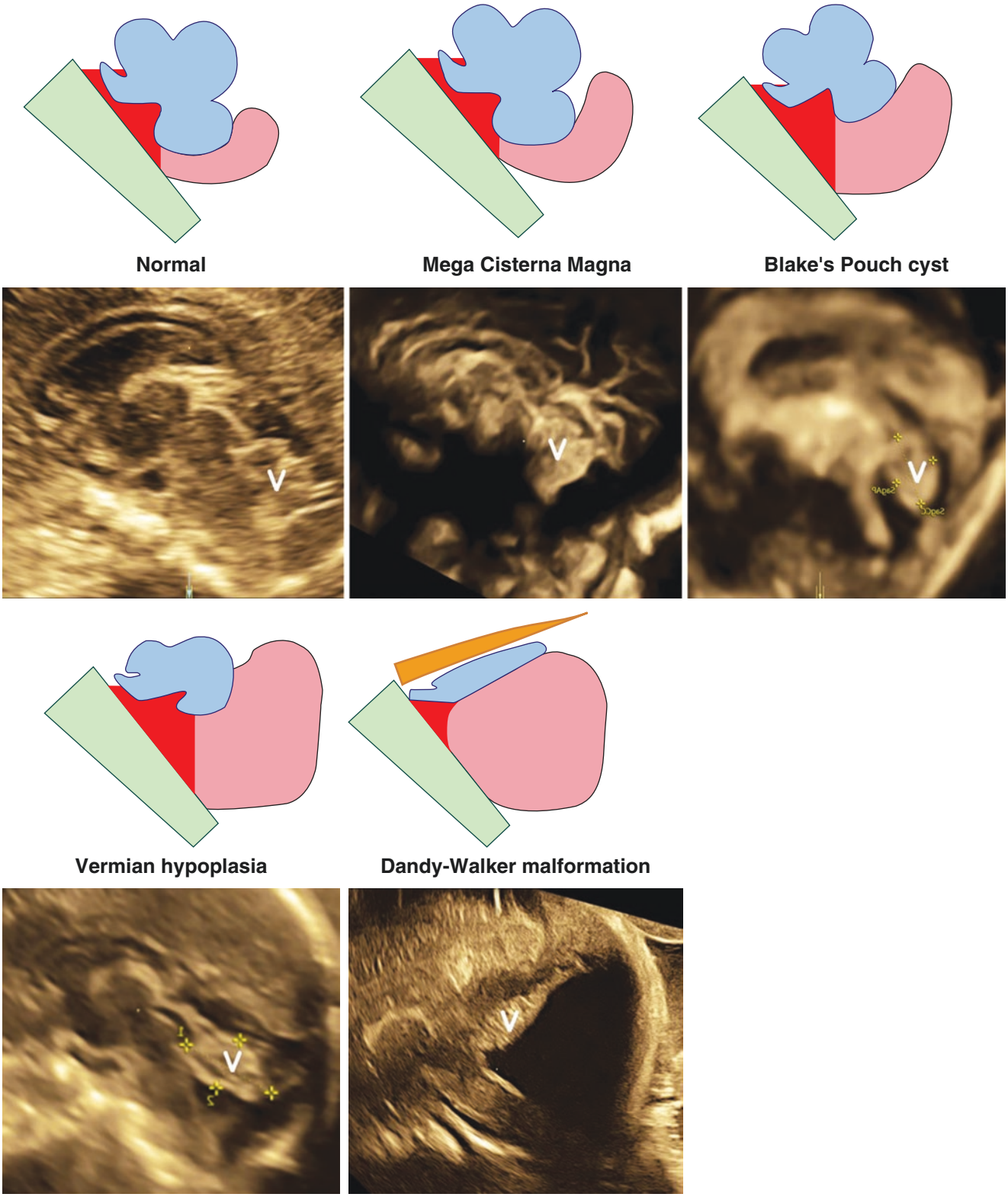

Fig. 5.1 Schematic diagrams and corresponding US midsagittal sections of the continuum of disorders that arise from progressive dilatation of the Blake's pouch. The fourth ventricle (red) seamlessly continues into the Blake's pouch (pink) inferior to the vermis (blue), in both normal and abnormal conditions. The brainstem is in green and the tentorium in orange. The vermis is marked 'V' in the US images

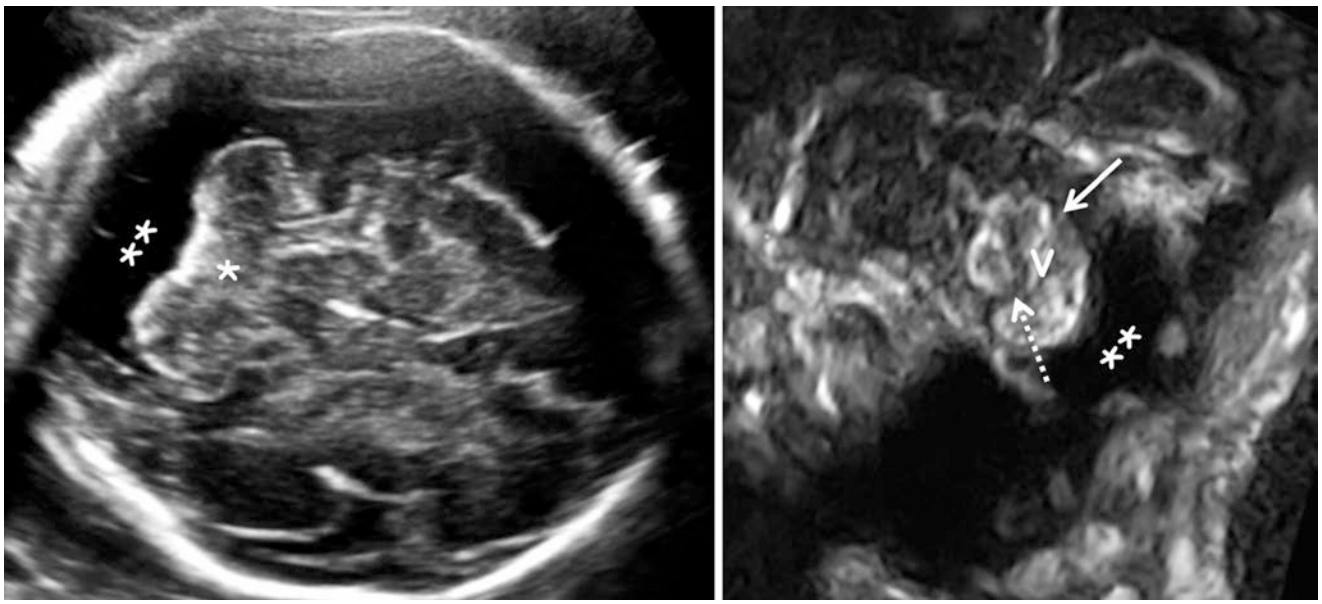

Fig. 5.2 29 weeks (TAS, 3D US) *mega cisterna magna* – axial transcerebellar section and 3D multiplanar midsagittal section – anteroposterior depth of cisterna magna is 1.5 cm (mega cisterna magna) (**), the vermis is intact (*) with no 'open fourth ventricle', primary fissure (solid arrow), fastigium (dotted arrow), vermis (V) is normal in position (not rotated), normal vermian size and shape

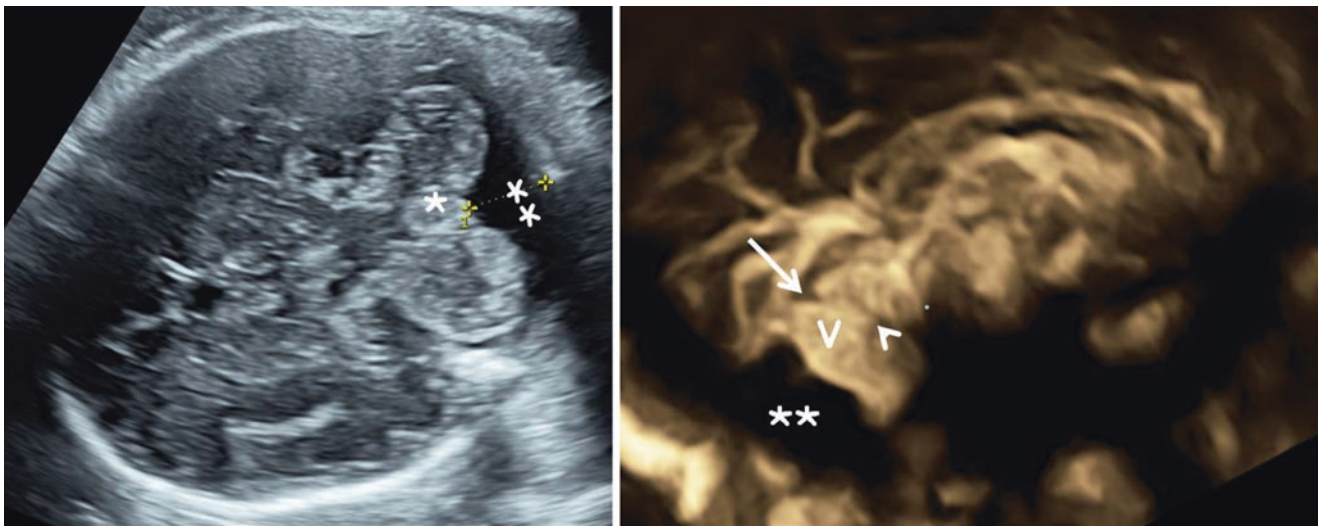

Fig. 5.3 31 weeks (TAS and 3D US) *mega cisterna magna* – axial transcerebellar section and 3D multiplanar midsagittal section with volume contrast imaging – the anteroposterior depth of cisterna magna is 1.4 cm (mega cisterna magna) (**), the vermis is intact (*) with no 'open fourth ventricle', primary fissure (solid arrow), fastigium (arrowhead), vermis (V) not rotated, normal vermian size and shape

5.2 Blake's Pouch Cyst

With increasing pressure in the Blake's pouch, the vermis is rotated (lower pole is lifted off the brainstem).

The ultrasound findings are as follows:

1. 'Open fourth ventricle' is seen in the axial transcerebellar section.
2. Vermian rotation is seen in the midsagittal section. The brainstem vermis angle is increased (23° ± 2.8°).
3. The vermian size and shape are normal in the midsagittal section (Figs. 5.4, 5.5 and 5.6a, b).
4. Blake's pouch cyst can regress (due to fenestration) with advancing gestational age. This results in de-rotation of the vermis and its return to a normal position (Fig. 5.6a, b).

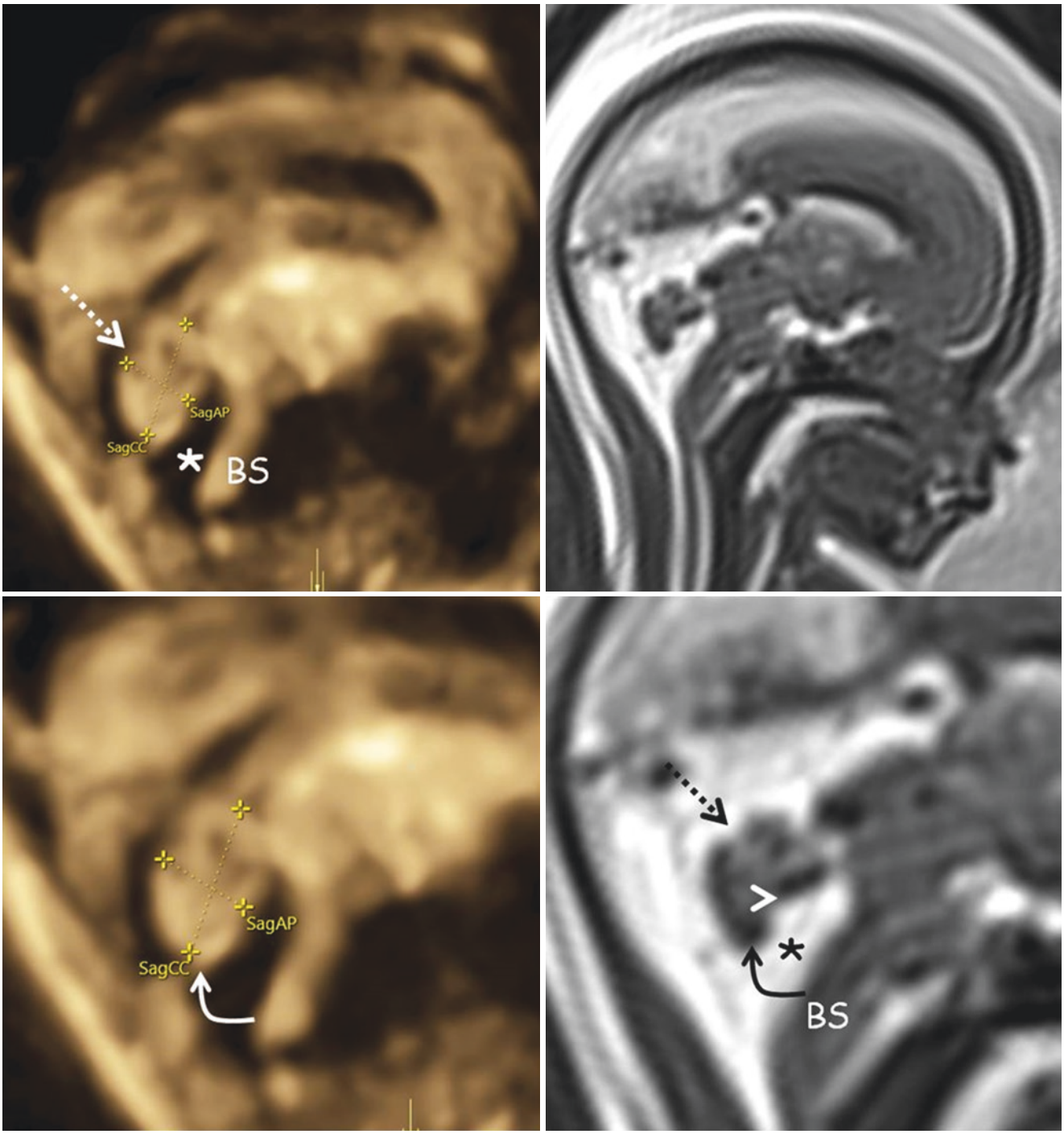

Fig. 5.4 20 weeks (TAS, 3D US and MRI) *Blake's pouch cyst* – 3D US and T2W midsagittal sections – fourth ventricle (*), normal size and shape of vermis (dotted arrow), vermian rotation (curved solid arrow), lower pole of vermis lifted off the brainstem (BS), fastigium (arrowhead). Note that the fourth ventricle continues imperceptibly into the Blake's pouch cyst at the inferior border of the vermis

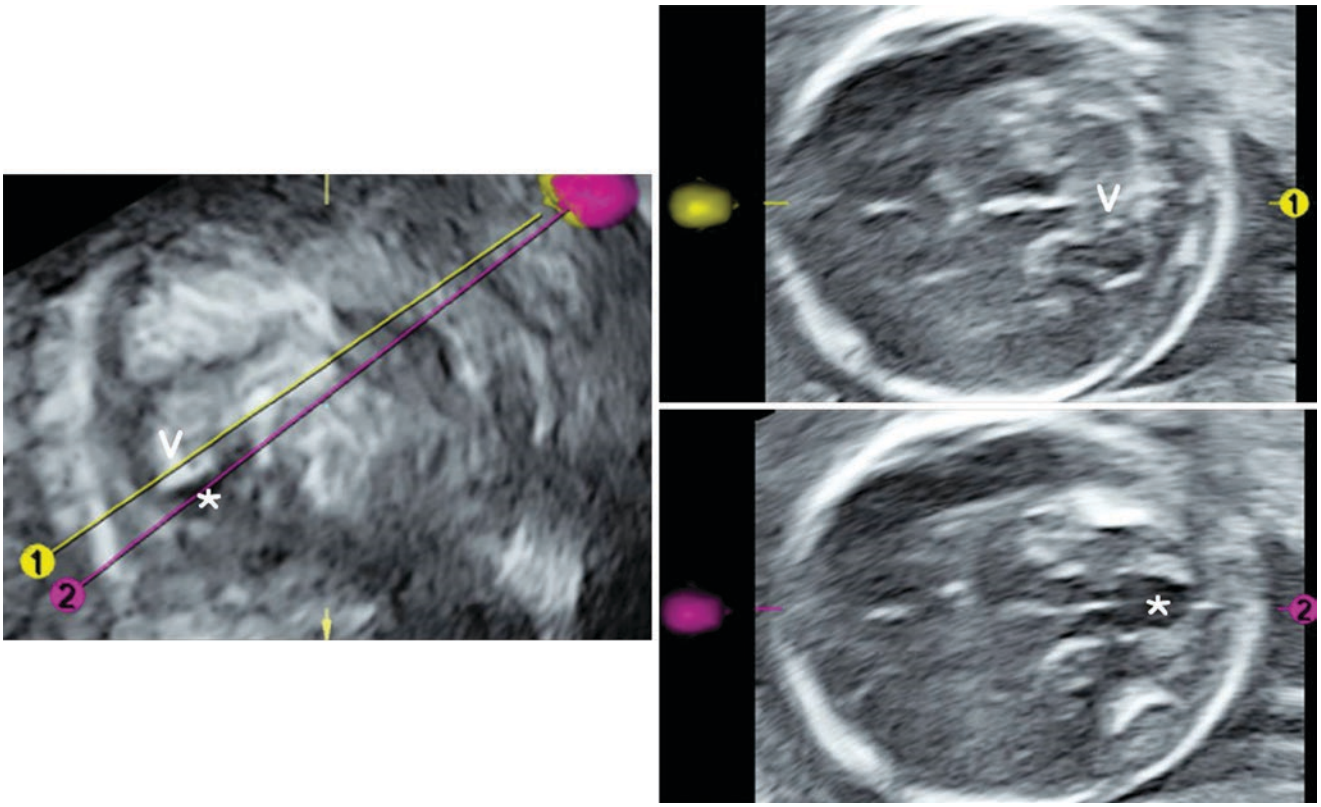

Fig. 5.5 20 weeks (TAS 3D omniview) *Blake's pouch cyst* – reference image is the midsagittal section (vermis is rotated but normal in shape and size) with semicoronal omniview planes through vermis (yellow line) and the fourth ventricle (pink line) – normal vermis (v) seen in the former section. 'Open fourth ventricle' (*) seen in the latter section

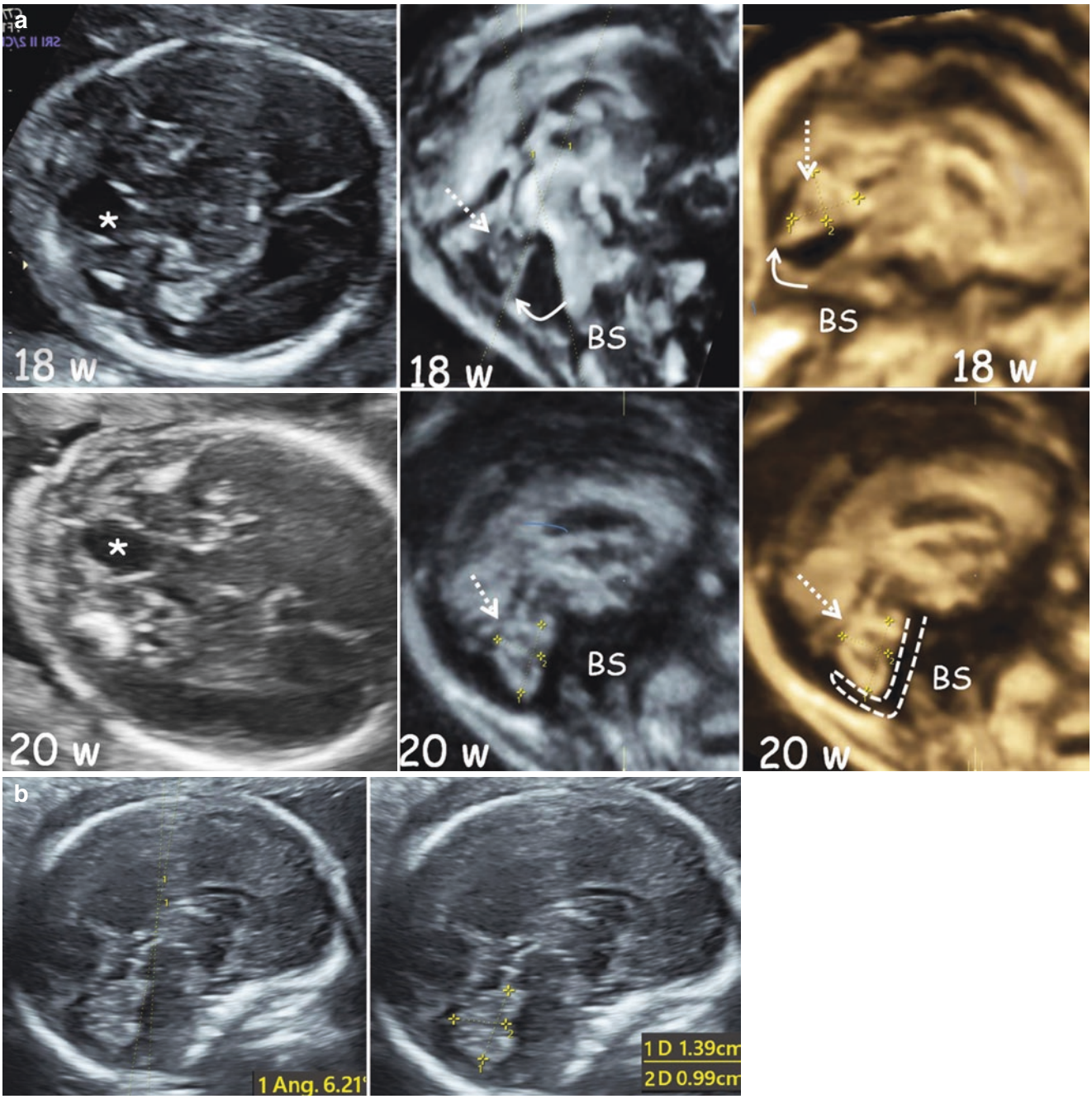

Fig. 5.6 (**a**) 18 and 20 weeks (TAS and 3D US) *Blake's pouch cyst* – axial transcerebellar and 3D midsagittal sections – open fourth ventricle on axial sections (*), normal size and shape of vermis (dotted arrows), vermian rotation, lower pole of vermis lifted off the brainstem (BS) (curved solid arrow). The brainstem vermis angle was 32°. The degree of rotation is decreased in the 20 weeks study as compared to the 18 weeks, fourth ventricle continuous with Blake's pouch cyst extending into the cisterna magna (dotted shape). (**b**) 24 weeks (TAS) *Blake's pouch cyst (regressed)* midsagittal sections – the vermis is now completely de-rotated. The brainstem vermis angle is 6° (normal)

5.3 Vermian Hypoplasia

As the pressure in the Blake's pouch increases further, it causes rotation and compression of the vermis resulting in hypoplasia.

The ultrasound findings are as follows:

1. 'Open fourth ventricle' is seen in the axial transcerebellar section.
2. In the midsagittal section, the vermis is small and rotated. The vermian cephalocaudal and anteroposterior dimensions are less than fifth percentile. The brainstem vermis angle is increased (35° ± 5.4°).
3. The vermis is misshapen. The kidney bean shaped, fastigium and primary fissure are not seen (Figs. 5.7, 5.8, 5.9 and 5.10).

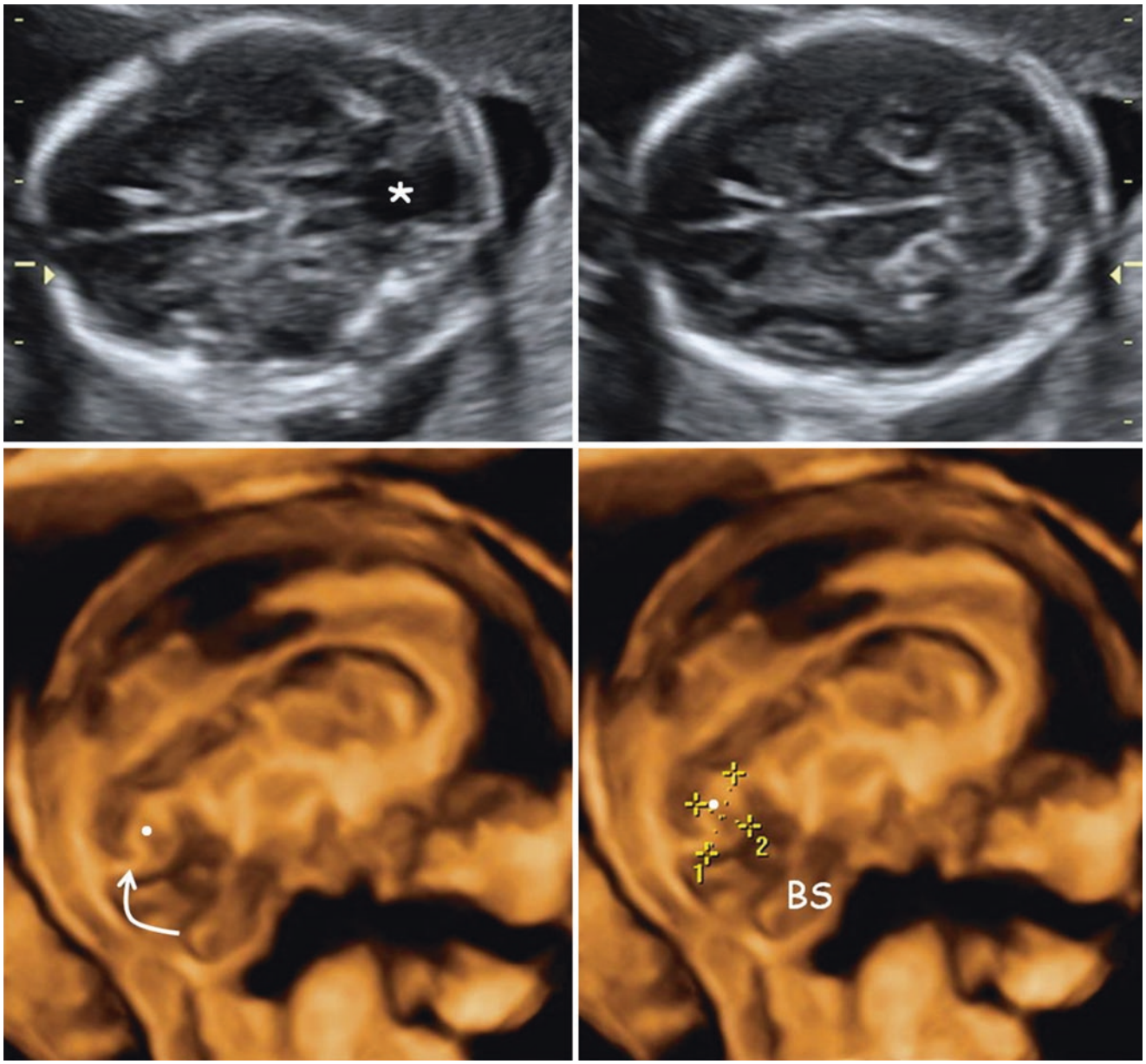

Fig. 5.7 20 weeks (TAS and 3D US) *vermian hypoplasia* – axial transcerebellar inferior and superior sections and 3D midsagittal section – open fourth ventricle (*) seen in the inferior axial section and not in the superior axial section, misshapen small (8 × 6 mm) vermis (dot), landmarks of fastigium and primary fissure not seen, rotation of vermis (curved solid arrow), brainstem (BS)

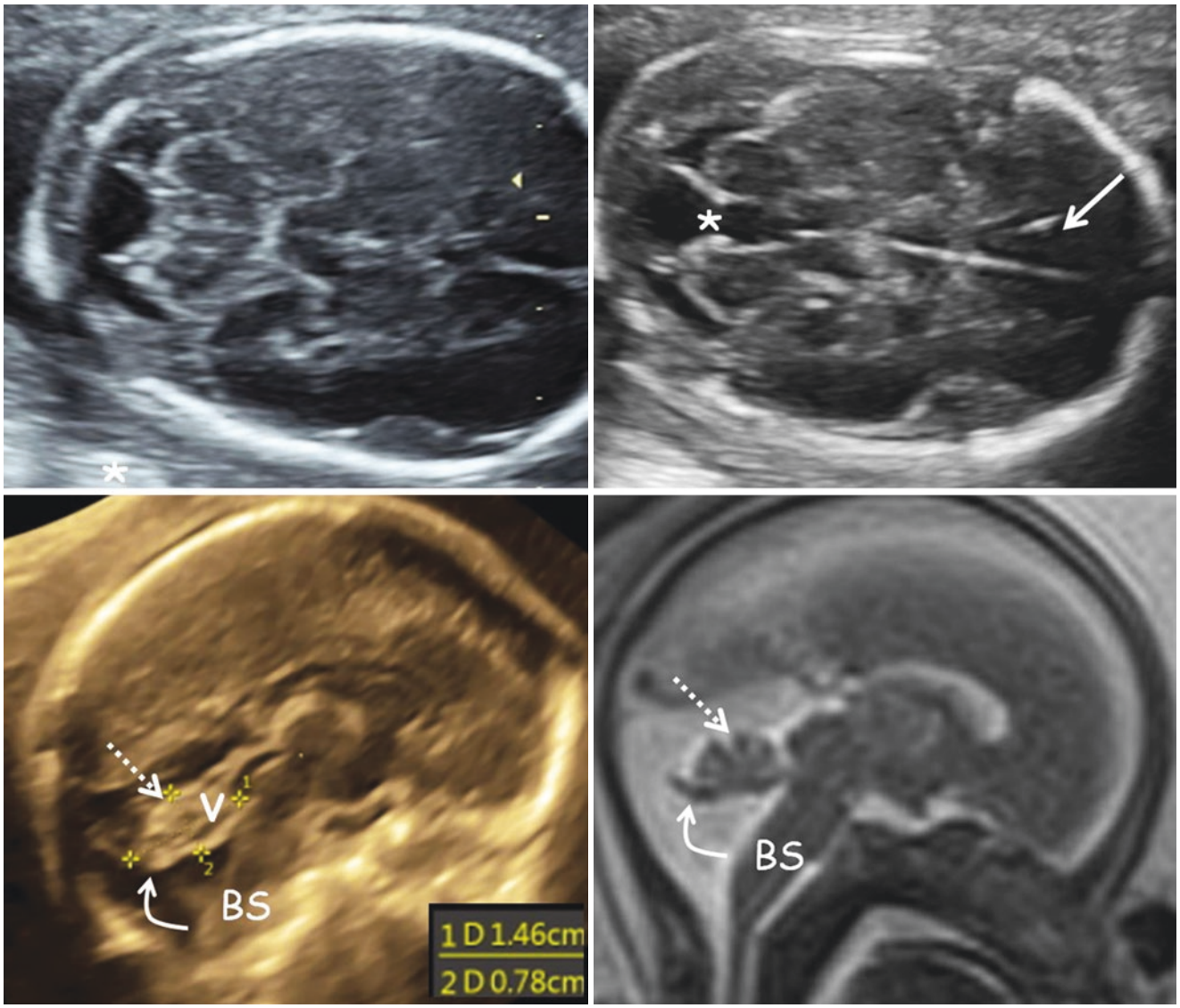

Fig. 5.8 22 weeks (TAS, 3D US and MRI) *vermian hypoplasia* – axial transcerebellar superior and inferior sections, 3D US and T2W midsagittal sections – open fourth ventricle on inferior axial section (*), vermis (V), primary fissure (dotted arrow), anterior lobe above the primary fissure is normal in size, posterior lobe below the primary fissure is small, vermian rotation, lower pole of vermis lifted off the brainstem (BS) (curved solid arrow). Brainstem-vermis angle is 30°

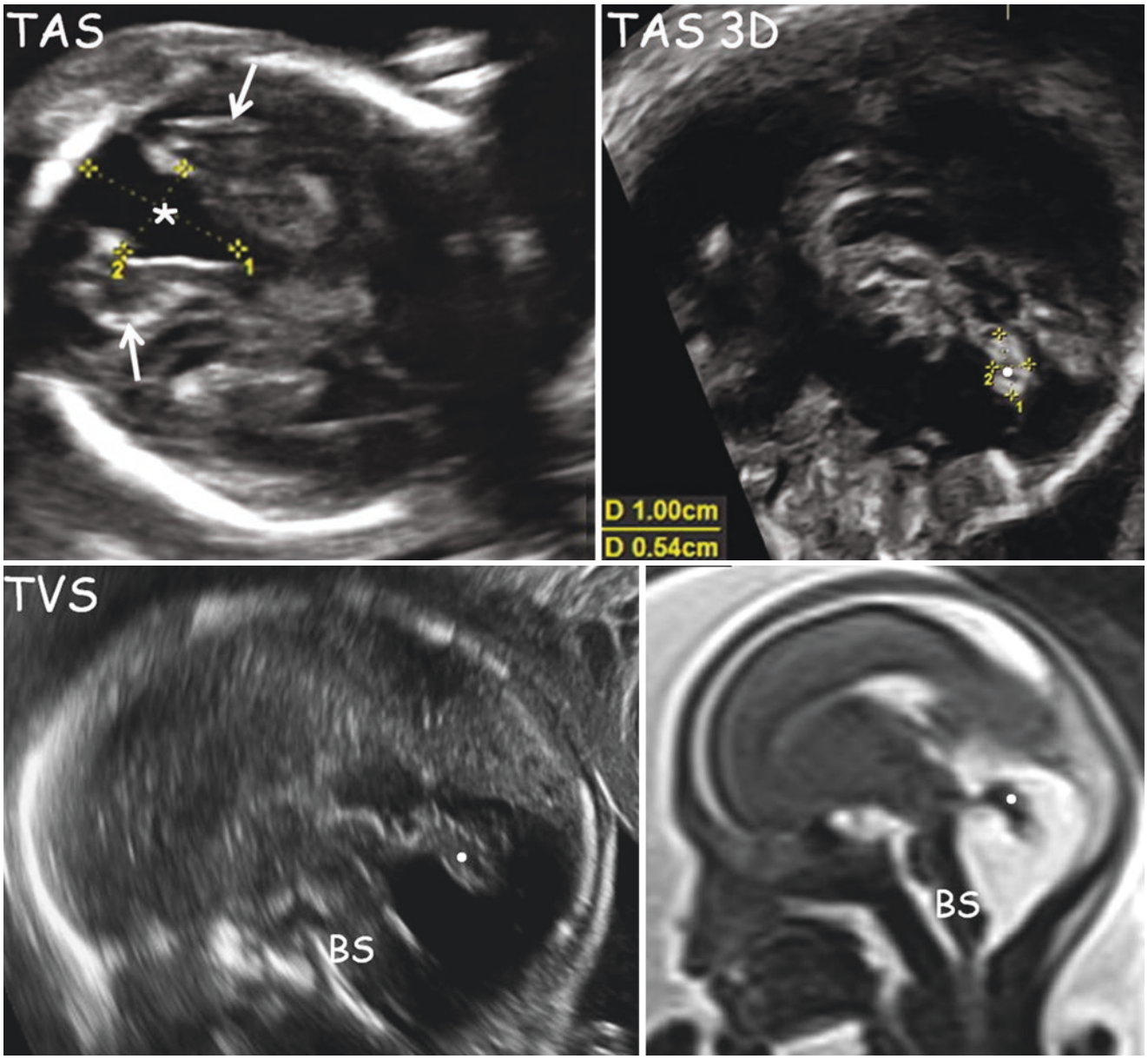

Fig. 5.9 22 weeks (TAS, 3D US, TVS and MRI) *vermian hypoplasia* – axial transcerebellar, 3D US, TVS and T2W midsagittal sections – open fourth ventricle (*) cerebellar hemispheres (solid arrows), small (10 × 5 mm) ovoid rotated vermis (dot), landmarks of fastigium and primary fissure are not seen, brainstem-vermis angle of 30°, brainstem (BS)

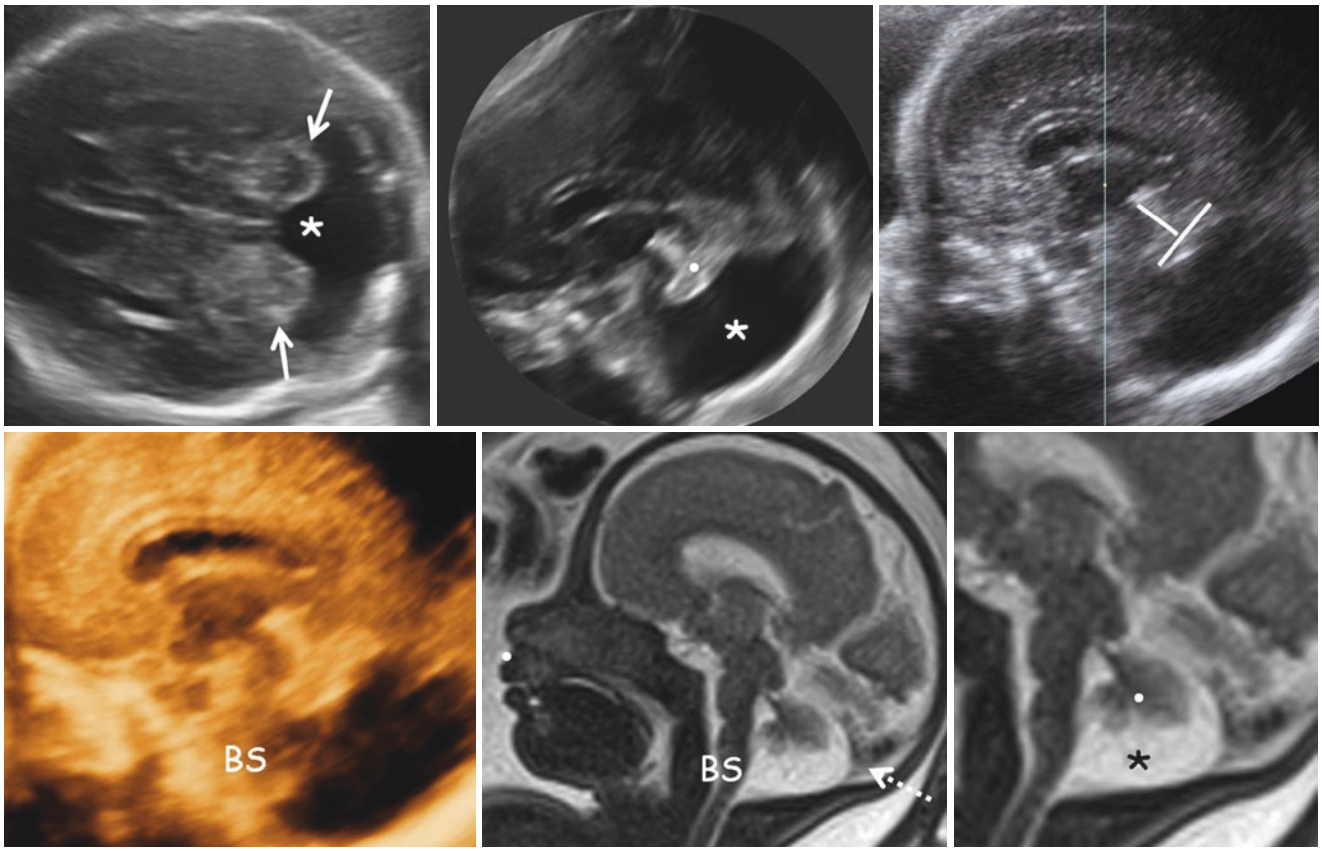

Fig. 5.10 28 weeks (TAS, 3D US and MRI) *vermian hypoplasia* – axial transcerebellar section, 2D, 3D multiplanar, 3D rendered and T2W midsagittal sections – open fourth ventricle (*), cerebellar hemispheres (solid arrows), misshapen, 'Y' shaped, small (13 × 16 mm) vermis (dot), landmarks of fastigium and primary fissure are absent, torcula and tentorium are not elevated (dotted arrow), brainstem (BS)

5.4 Dandy-Walker Malformation

Ultimately, the Blake's pouch becomes extremely large and tense. Such a cyst grossly elevates the vermis and the tentorium. The vermis is severely compressed against the tentorium. The cyst is a composite of the dilated fourth ventricle and the large contiguous Blake's pouch.

The ultrasound findings are as follows:

1. A large midline cyst is seen splaying and compressing the cerebellar hemispheres in the transcerebellar axial section.
2. The posterior fossa is expanded.
3. The vermis is compressed, flattened and elevated by the cyst in the midsagittal section (Figs. 5.11 and 5.12).
4. The torcula, transverse sinuses and tentorium are elevated. Torcular elevation can be seen on fetal MRI.
5. The largest brainstem vermis angle is encountered in DWM (63.5° ± 17.6°) and reflects tentorial elevation.
6. Associated frank lateral ventriculomegaly may be seen.
7. DWM may be found in association with Meckel-Gruber, Aicardi and Walker-Warburg syndromes. It may be associated with chromosomal abnormalities, and hence fetal karyotyping or chromosomal microarray is indicated. Associated sporadic intracranial and extracranial abnormalities have to be looked for.

Distinguishing between BPC and VH can be challenging. The vermis is rotated in both conditions. The key to the diagnosis is the vermian morphology. The size and shape of the vermis are normal in BPC and abnormal in VH. A good midsagittal section is crucial for assessment of the vermis. Without a midsagittal section, it is not possible to arrive at a specific diagnosis.

Prognosis is based on the presence of normal vermis (size and shape) on the midsagittal section. Presence of vermis with normal size and shape as in mega cisterna magna and Blake's pouch cyst (provided they are isolated findings) are associated with normal neurodevelopmental outcome. Abnormal vermian size and shape as in vermian hypoplasia and Dandy-Walker malformation are associated with abnormal neurodevelopmental outcome.

The following table summarises the findings in the continuum of findings seen in mega cisterna magna, Blake's pouch cyst, vermian hypoplasia and Dandy-Walker malformation.

Diagnosis	Vermian size	Vermian form	Vermian rotation	Cisterna magna	Tentorial level
MCM	Normal	Normal	Absent	Large	Normal
BPC	Normal	Normal	Mild	Normal/large	Normal
VH	Small	Abnormal	Moderate	Large	Normal
DWM	Compressed	Flattened	Gross	Very large PCF expansion	Elevated

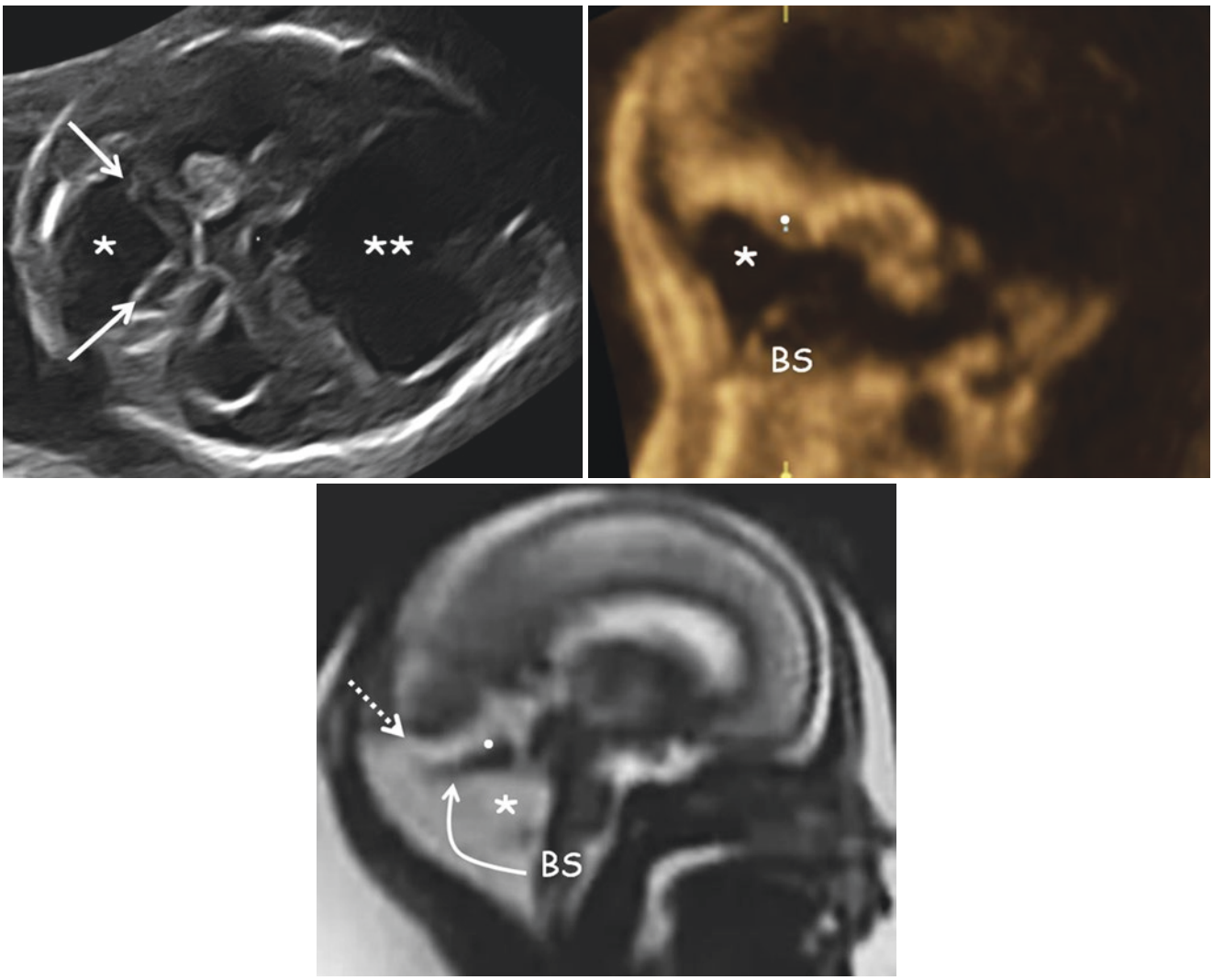

Fig. 5.11 21 weeks (TAS 3D US and MRI) *Dandy-Walker malformation* – 3D multiplanar axial transcerebellar, 3D rendered and T2W midsagittal sections – severe lateral ventricular dilatation (**); midline posterior cranial fossa cystic lesion (*) splaying and compressing the cerebellar hemispheres (solid arrows); flattened, compressed and severely rotated (curved solid arrow) vermis (dot); landmarksv of fastigium and primary fissure not seen; tentorium is elevated (dotted arrow); brainstem (BS). Brainstem-vermis angle is 81°

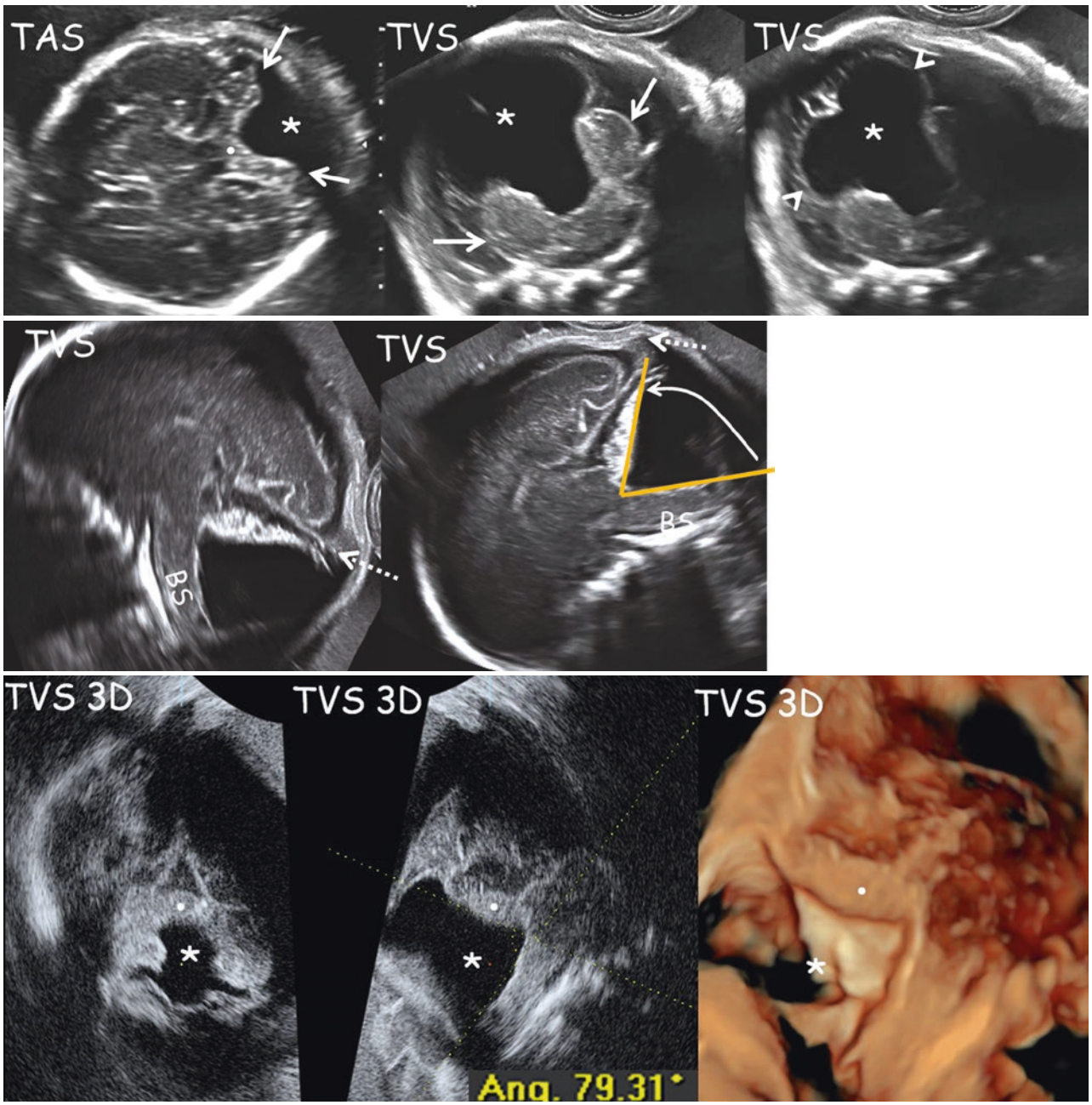

Fig. 5.12 28 weeks (TAS, TVS and 3D US) *Dandy-Walker malformation* – axial transcerebellar, magnified axial transcerebellar, midsagittal, 3D multiplanar coronal transcerebellar and rendered midsagittal sections – midline posterior cranial fossa cystic lesion (*) splaying and compressing the cerebellar hemispheres (solid arrows); walls of the Dandy-Walker cyst (arrowheads); flattened, compressed and grossly rotated (curved solid arrow) vermis (dot); landmarks of fastigium and primary fissure are absent; torcula and tentorium are elevated (dotted arrow); brainstem (BS); brainstem-vermis angle is 80°

5.5 Cerebellar Hypoplasia

A small but normal-shaped cerebellum is termed hypoplastic.

The ultrasound findings are as follows:

1. The cerebellum in the transcerebellar axial section is normal in shape but small in size. Transverse cerebellar diameter (TCD) is lesser than fifth percentile (Fig. 5.13).
2. The cisterna magna appears apparently large.
3. Borderline small TCD is difficult to interpret. Decreasing percentiles on serial TCD measurements at two weekly intervals confirm hypoplasia.
4. Diagnosis is possible only in the late second or third trimesters.
5. Associated intracranial or extracranial anomalies are common and should be looked for. Cerebellar hypoplasia may be associated with chromosomal abnormalities, syndromes and fetal infections.

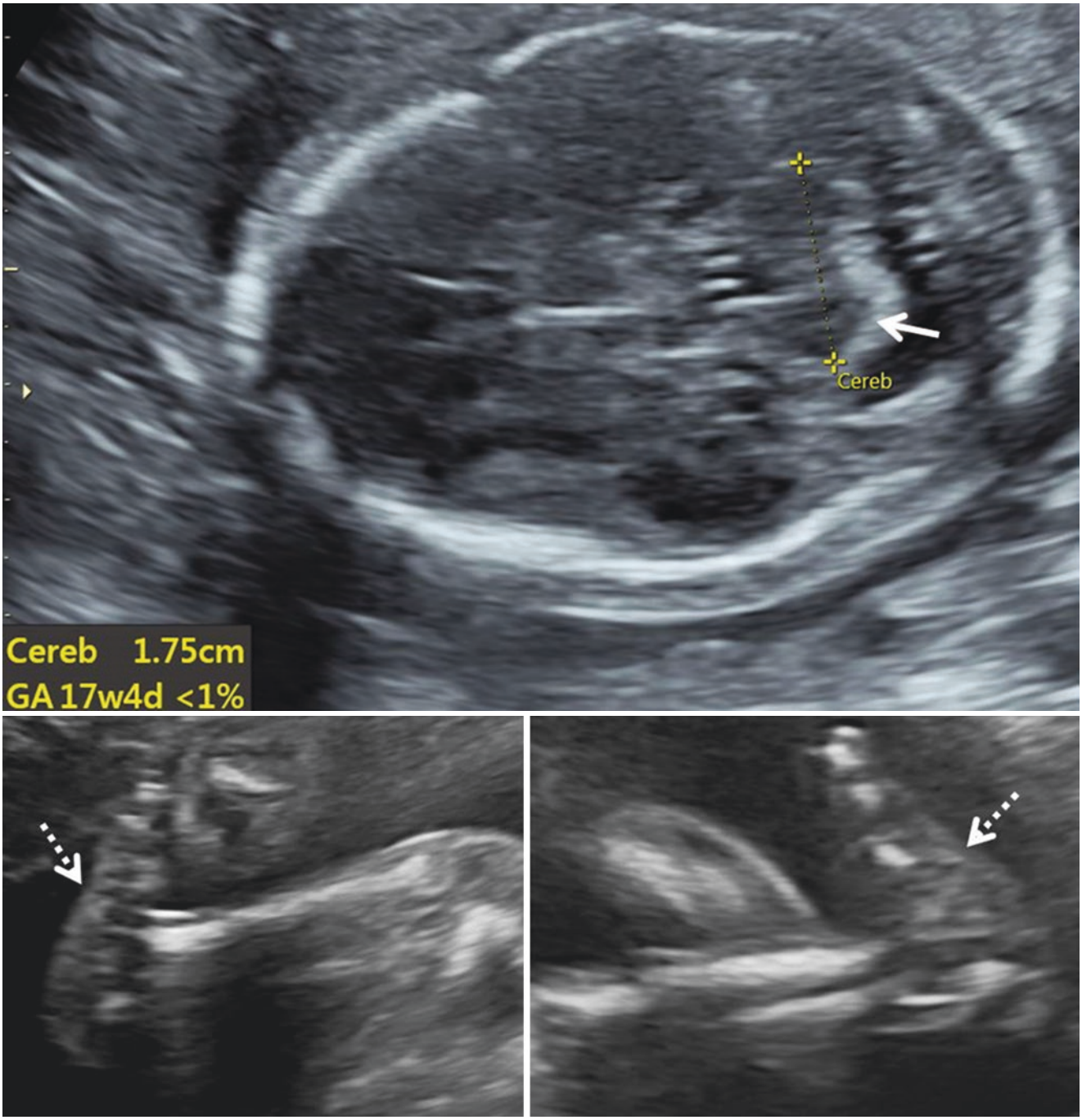

Fig. 5.13 21 weeks (TAS) *cerebellar hypoplasia* – axial transcerebellar section of the cranium and sagittal section of both legs – small cerebellum (solid arrow) less than fifth percentile transverse cerebellar diameter, bilateral rocker-bottom feet (dotted arrows)

6. Unilateral cerebellar hypoplasia (Fig. 5.14) may be due to a destructive process (ischemia or infection). Appearances may change with time. If there is no progressive change and the vermis is normal, the outcome is generally good. Unilateral cerebellar hypoplasia can be a part of PHACE syndrome (haemangioma, posterior fossa, cardiac and eye anomalies).
7. Cerebellar hypoplasia is also associated with an autosomal recessive group of neurodegenerative disorders termed pontocerebellar hypoplasia (PCH, most common type is type II caused by TSEN54 mutation). In addition to cerebellar hypoplasia, there is hypoplasia of the brainstem, particularly of the pons. In the midsagittal section, the ventral belly of the pons is flat. Fetal MRI confirms the brainstem hypoplasia and cerebellar pathology (Fig. 5.15a, b). Neurogenic arthrogrypotic sequelae, fetal seizures and polyhydramnios may be seen particularly in late gestation. Prognosis is poor. Targeted neurosonogram with serial TCD measurements is indicated in cases with previous pregnancies with PCH. Molecular testing for the specific genetic mutation is necessary for early prenatal diagnosis in subsequent pregnancies.

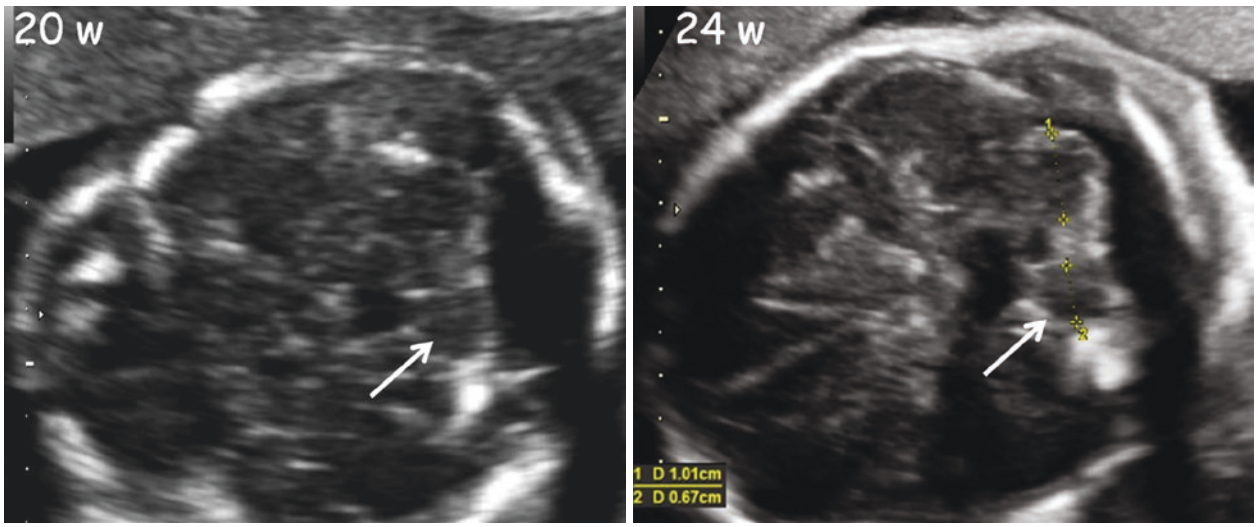

Fig. 5.14 20 and 24 weeks (TAS) *unilateral left cerebellar hemispheric hypoplasia* – axial transcerebellar sections – smaller left cerebellar hemisphere (solid arrows), compared to right, cisterna magna is apparently large on the left side. The vermis was normal. No associated anomalies were noted

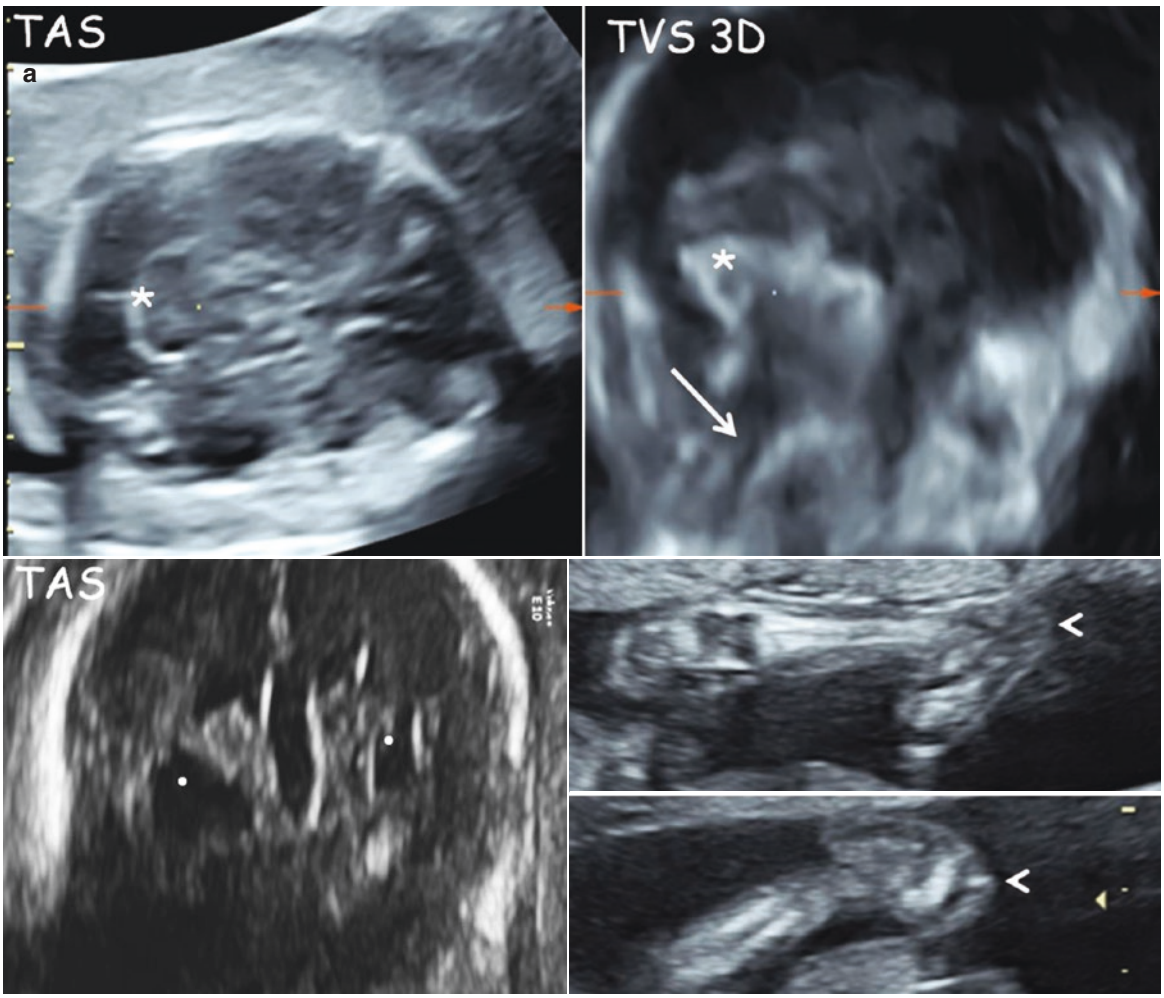

Fig. 5.15 (**a**) 22 weeks (TAS, 3D US and MRI) *pontocerebellar hypoplasia* – axial transcerebellar, 3D multiplanar midsagittal, coronal transcaudate sections of cranium and coronal sections of legs – cerebellum is small (*), brainstem (solid arrow) is thin, hypoplastic, pontine belly is not seen, bilateral periventricular cysts (dots), right rocker-bottom foot and left talipes equinovarus (arrowheads). (**b**) 22 weeks (TAS, 3D US and MRI) *pontocerebellar hypoplasia* – T2W axial transventricular, axial transcerebellar and midsagittal sections – cerebellum is small (*), brainstem (solid arrow) is thin, hypoplastic, pontine belly is not seen, bilateral periventricular cysts (dots)

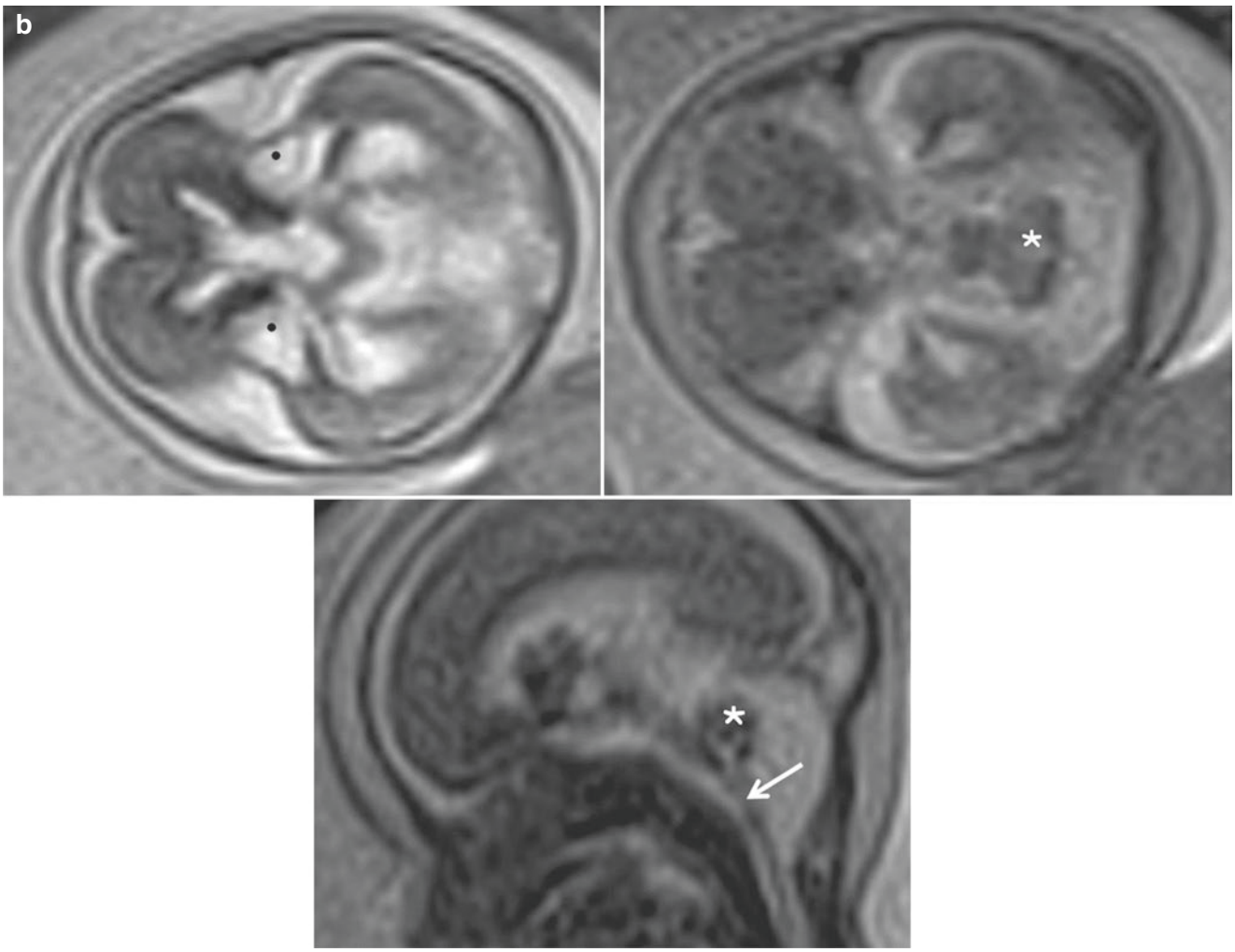

Fig. 5.15 (continued)

5.6 Rhombencephalosynapsis

Rhombencephalosynapsis is characterised by the absence of the vermis and anatomical continuity of the hemispheres.

The ultrasound findings are as follows:

1. The cerebellum is a single mass and appears globular or triangular in shape instead of the normal dumbbell shape (Figs. 5.16, 5.17a, b, 5.18 and 5.19).
2. The vermis is absent, and the cerebellar hemispheres are in continuity with each other across the midline. This is seen as absence of the midline 'handle' of the dumbbell-shaped cerebellum in the transcerebellar axial section (Fig. 5.18).
3. The transverse cerebellar diameter is less than normal.
4. The cisterna magna loses its typical lozenge shape (Fig. 5.16).
5. Rhombencephalosynapsis occurs as a spectrum, varying from subtle absence of vermis (Fig. 5.17a, b) to a small globular cerebellum (Fig. 5.16).
6. On a tangential section through the superior cerebellar surface, the folia are seen to run across the midline from one side to the other (Fig. 5.17a).
7. The vermis is not seen as a hyperechoic kidney bean-shaped structure on midsagittal sections. Instead the cerebellar hemisphere is seen as a larger and hypoechoic 'vermis like structure' without the primary fissure and a pointed fastigium.

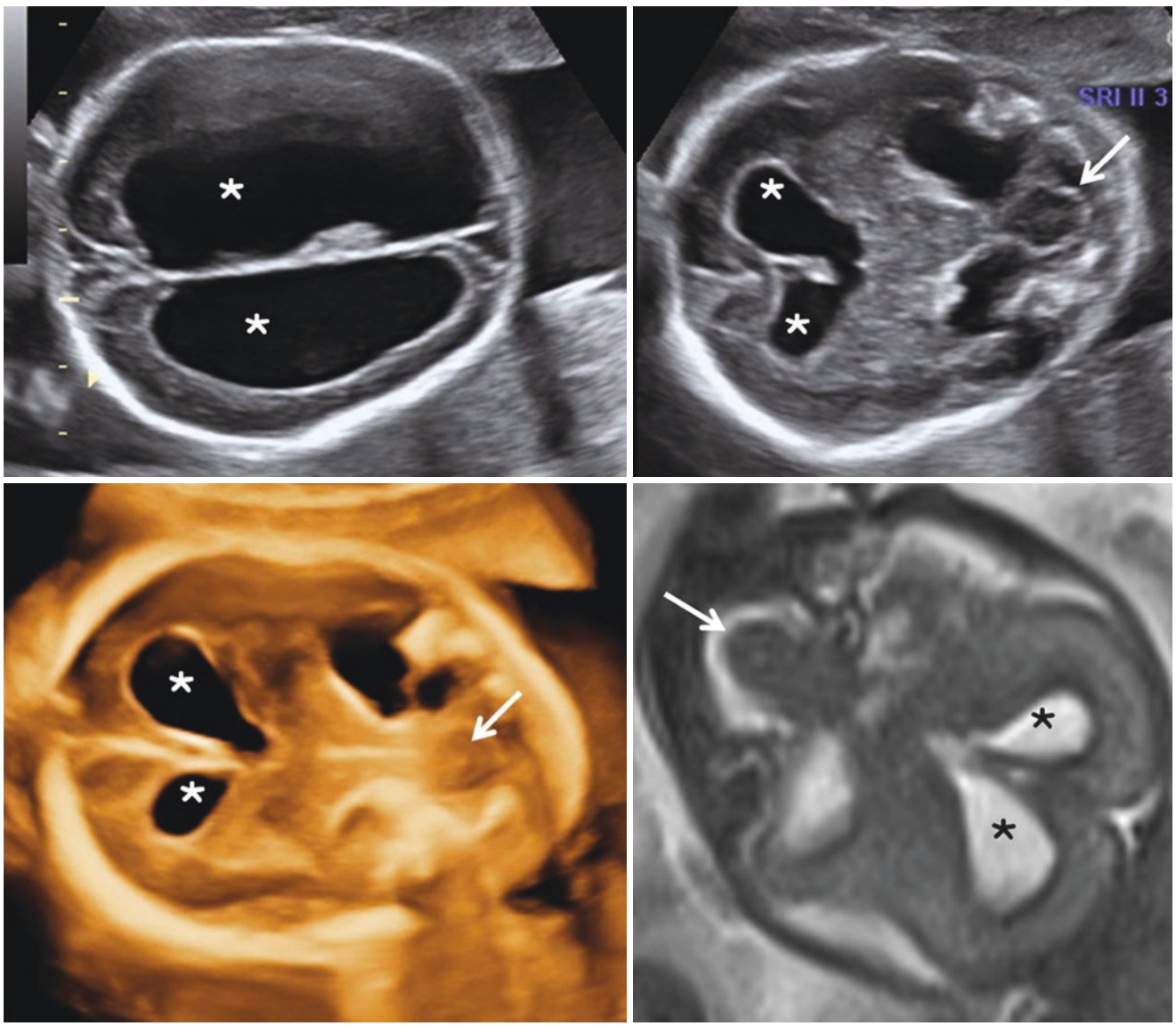

Fig. 5.16 24 weeks (TAS, 3D US and MRI) *rhombencephalosynapsis* – axial transventricular and transcerebellar sections, 3D rendered and T2W axial transcerebellar sections – bilateral gross lateral ventriculomegaly (*), small globular cerebellum (solid arrow)

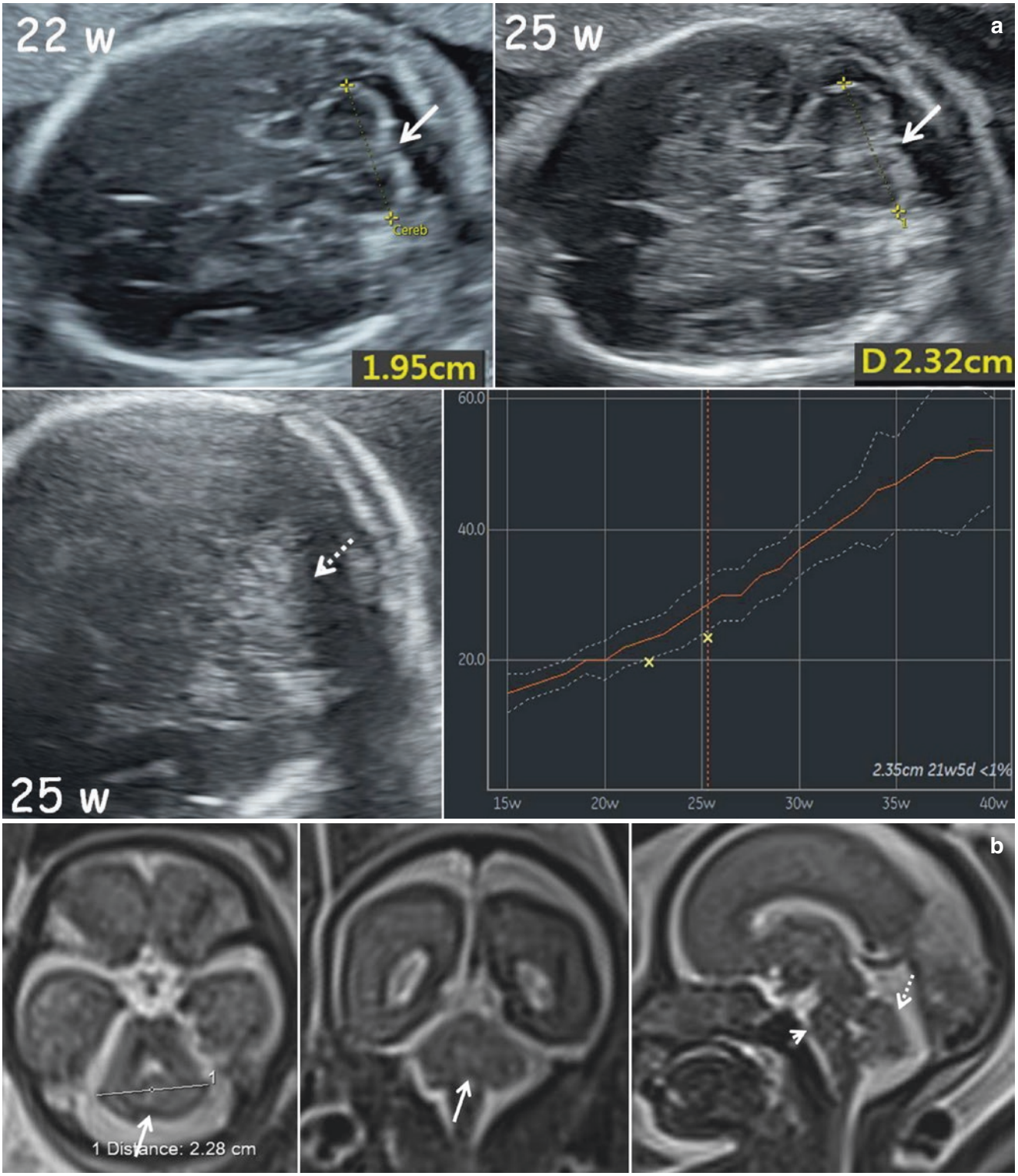

Fig. 5.17 (**a**) 22 and 25 weeks (TAS and MRI) *rhombencephalosynapsis* – axial transcerebellar and tangential posterior cerebellar sections – cerebellar hemispheres are continuous with each other across the midline with absence of vermis (solid arrow), 'handle' of the dumbbell is not seen, folia run across the cerebellum from side to side (dotted arrow), cerebellum is small with transverse cerebellar diameter below fifth percentile in both the studies. (**b**) 25 weeks (TAS and MRI) *rhombencephalosynapsis* – T2W axial and coronal transcerebellar and midsagittal sections – small, globular cerebellum with no vermis in the midline (solid arrow), cerebellar hemisphere in midsagittal plane (dotted arrow), pontine belly is not seen (arrowhead) indicating pontine hypoplasia

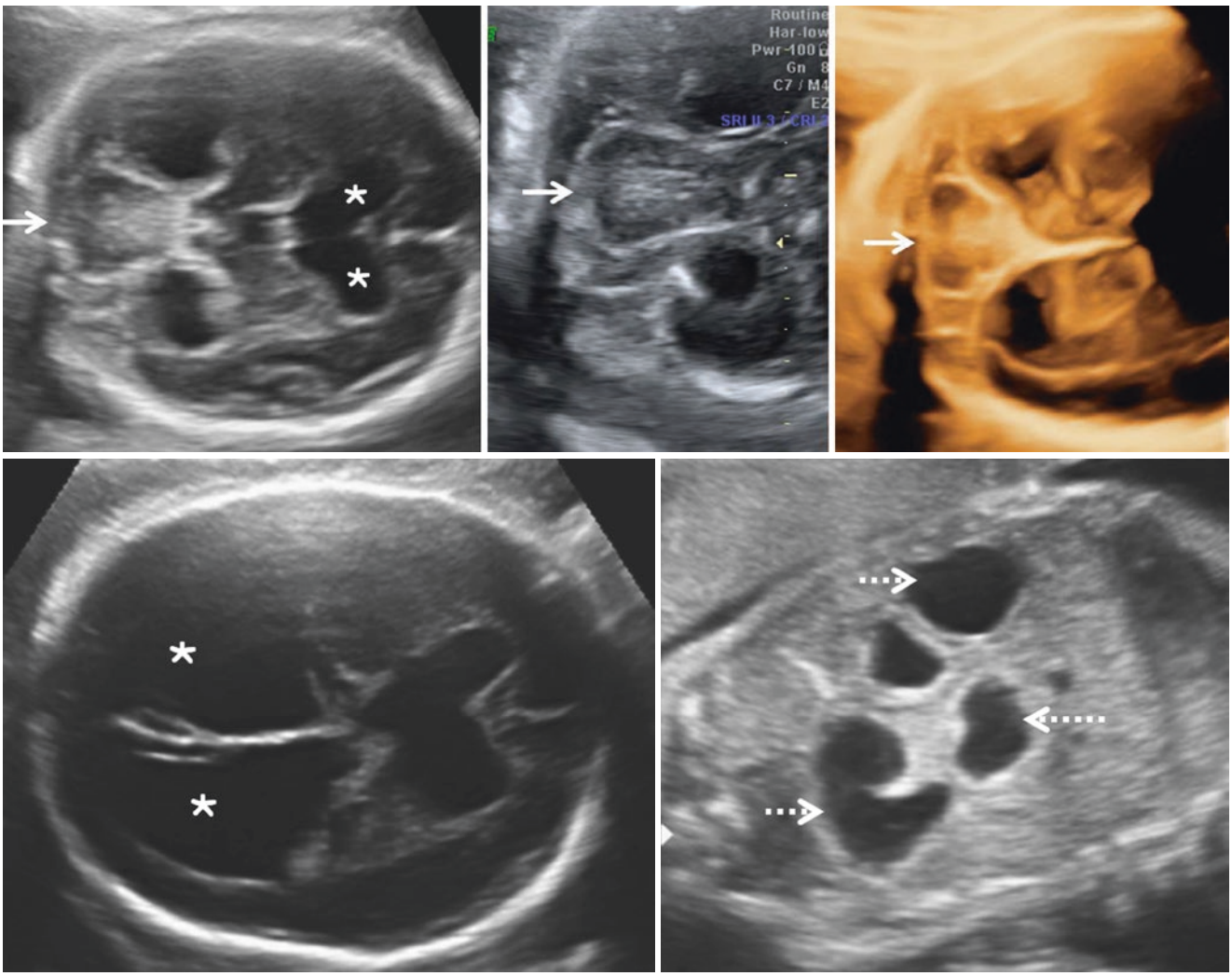

Fig. 5.18 25 weeks (TAS) *rhombencephalosynapsis* – axial transcerebellar section with magnification, 3D rendered transcerebellar section, axial transventricular section and coronal abdominal section – cerebellar hemispheres are continuous with each other across the midline with the absence of vermis (solid arrow), 'handle' of the dumbbell is not seen, the cerebellum is globular and the transverse cerebellar diameter is small, there is gross bilateral lateral ventriculomegaly (*), dilated stomach, duodenum and first loop of jejunum due to proximal jejunal atresia (dotted arrow)

8. The fourth ventricle in the transcerebellar axial section appears wider than longer normally. In cerebellar abnormalities (rhombencephalosynapsis, pontocerebellar hypoplasia, Joubert syndrome and related disorders), the fourth ventricle is longer than wider. The fourth ventricle index is normally more than one. In cerebellar abnormality the index is less than one (Fig. 5.19).
9. Rhombencephalosynapsis may in a way be considered as holorhombencephaly. It is a rare anomaly. Associated hydrocephalus, agenesis of corpus callosum, uncleaved thalami, holoprosencephaly and deficiency of other midline structures (optic chiasma) may be seen.

5.7 Joubert Syndrome and Related Cerebellar Disorders

These disorders constitute an autosomal recessive group called ciliopathies. The findings include vermian hypoplasia and 'molar tooth' sign. Joubert syndrome presents as ataxia, developmental delay, abnormal eye movements, tachypnea-apnea spells, retinal coloboma, hyperechoic kidneys and polydactyly. The other syndromes in this group include COACH (coloboma, oligophrenia, ataxia, cerebellar hypoplasia), CORS (cerebello-oculo-renal) and OFD VI (orofaciodigital).

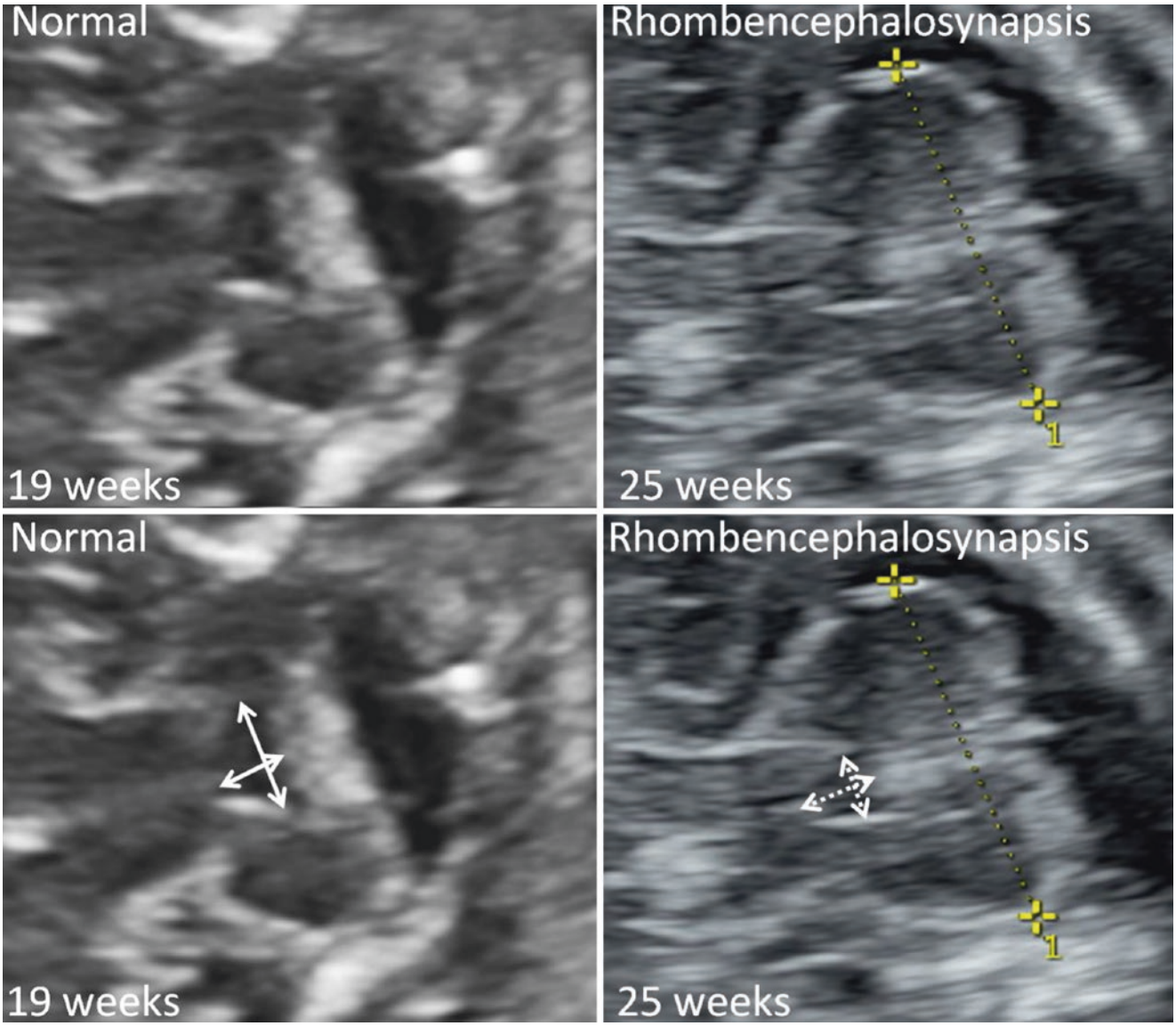

Fig. 5.19 19 and 25 weeks *fourth ventricle index (4VI) – normal and rhombencephalosynapsis* – magnified transcerebellar axial sections – laterolateral (LL) dimension is larger than the anteroposterior (AP) dimension normally yielding a 4VI of greater than one (solid arrows), the LL dimension is lesser than the AP dimension in rhombencephalosynapsis yielding a 4VI of lesser than one (dotted arrows). 4VI = LL dimension/AP dimension

The ultrasound findings are as follows:

1. Increased intracranial translucency (more than 95th percentile) is seen in the 11–14 weeks scan) (Fig. 5.20a, b).
2. 'Open fourth ventricle' is seen in the axial transcerebellar section in the 18–23 weeks US examination. The floor of the fourth ventricle is pointed anteriorly due to absence of decussation of the superior cerebellar peduncles (Figs. 5.20a, b and 5.21a, b).
3. Vermis is hypoplastic or absent. The kidney bean shape and the primary fissure are not seen in the midsagittal section (Fig. 5.22a, b).
4. Molar tooth sign is seen in the axial transcerebellar section. This is due to a combination of deep interpeduncular fossa and elongated superior cerebellar peduncles (Fig. 5.20b). This sign may be difficult to recognise on prenatal ultrasound. It is better seen on fetal MRI (T2-weighted imaging).

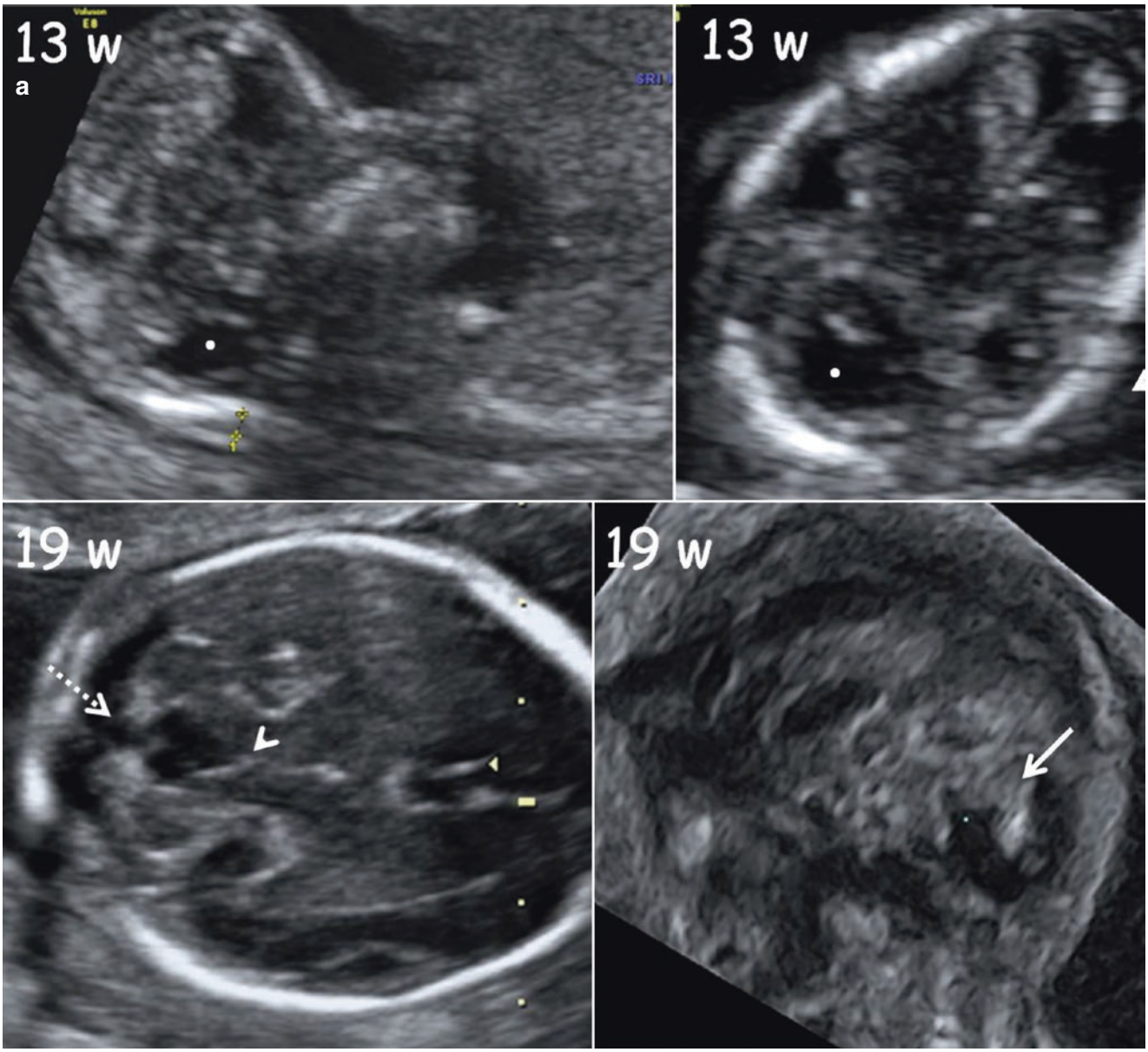

Fig. 5.20 (**a**) Third-degree consanguineous couple with an 11-year-old child with *Joubert syndrome* – 13 and 19 weeks (TAS) midsagittal and axial transcerebellar sections at 13 weeks, axial transcerebellar and midsagittal sections at 19 weeks – increased intracranial translucency (dot), normal brainstem, 'open fourth ventricle' (dotted arrow), floor of the fourth ventricle is pointed anteriorly (arrowhead), vermis is small and rotated (solid arrow). The molar tooth sign seen in the axial transcerebellar section is shown in the following figure. (**b**) Third-degree consanguineous couple with an 11-year-old child with *Joubert syndrome* – 19 weeks (TAS) axial transcerebellar section – deep interpeduncular cistern (dotted arrow), elongated superior cerebellar peduncles (solid arrows) constitute the 'molar tooth' sign. These findings confirm recurrence of *Joubert syndrome*

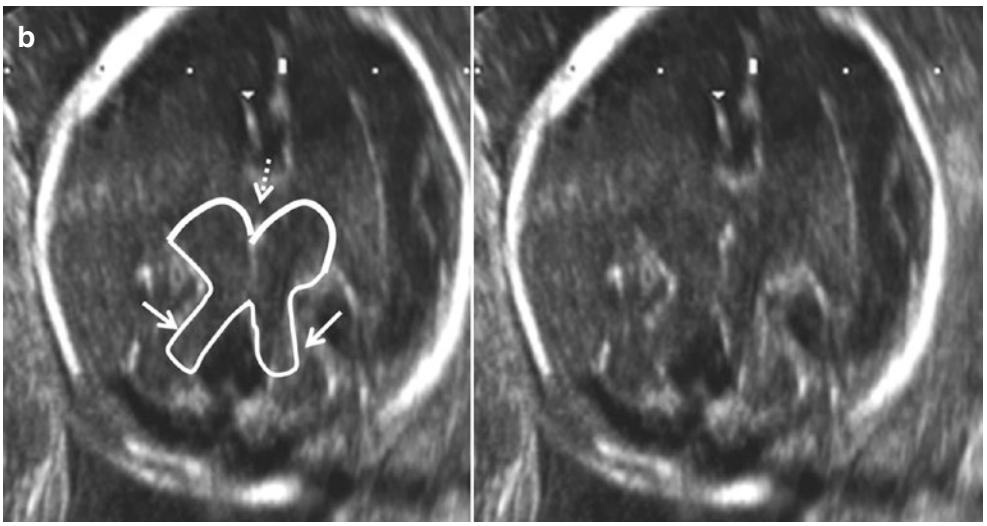

Fig. 5.20 (continued)

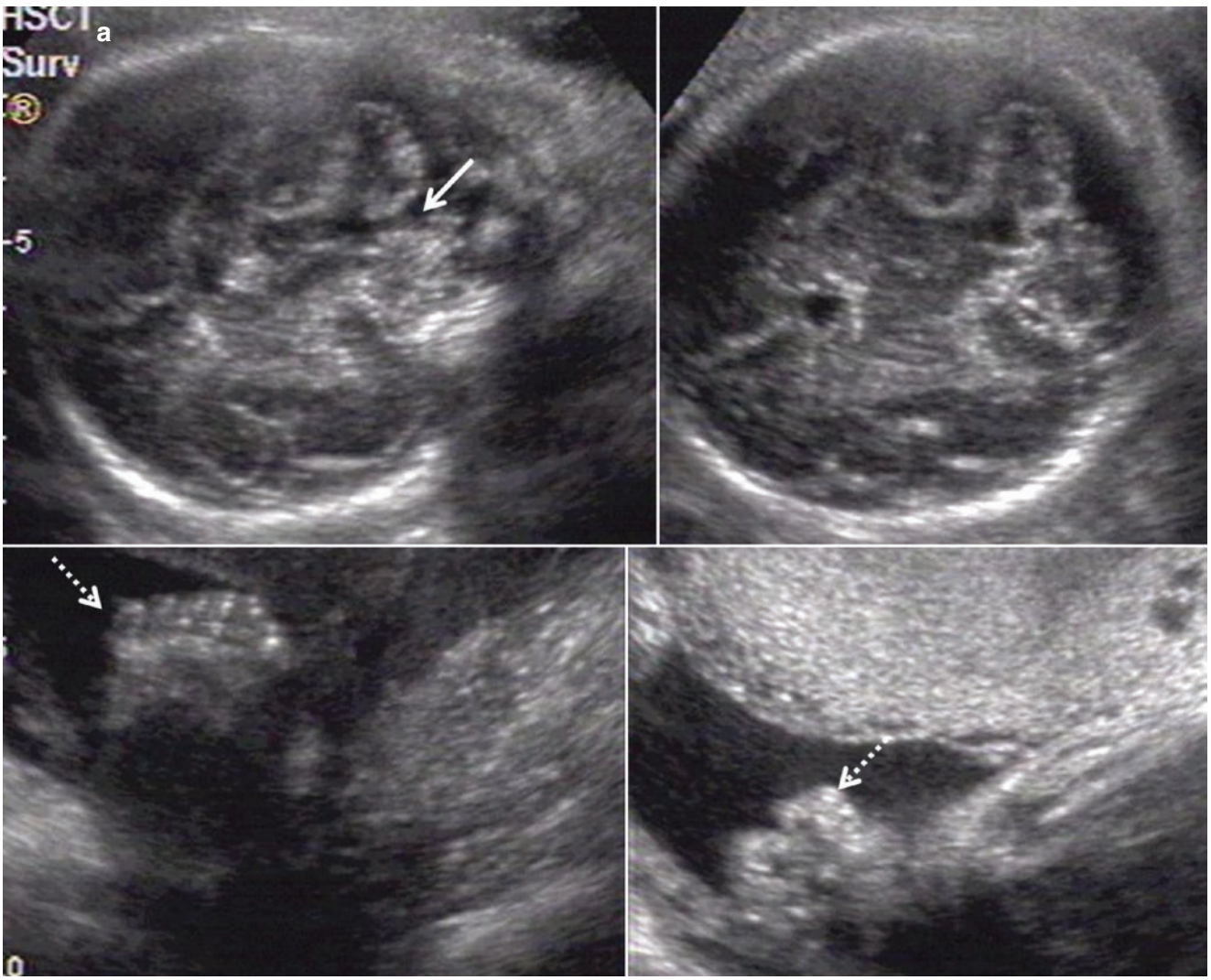

Fig. 5.21 (**a**) 26 weeks (TAS and MRI) *Joubert syndrome* – transcerebellar axial section (inferior and superior), coronal sections of the left foot and hand – 'open' fourth ventricle (solid arrow), postaxial polydactyly (dotted arrows) *Joubert syndrome* suspected due to these findings. MRI findings follow. (**b**) 26 weeks (fetal and postnatal MRI) *Joubert syndrome* – T2W fetal transcerebellar axial section, postnatal picture of polydactyly, T2W and T1W postnatal axial transcerebellar sections at 4 months of age – no 'molar tooth' sign seen (dotted arrow), postnatal picture of polydactyly. At 4 months MRI was done as nystagmoid movements of the eyes were noticed. 'Molar tooth' sign (solid arrows) seen confirming *Joubert syndrome*. This is an example of evolution of fetal findings

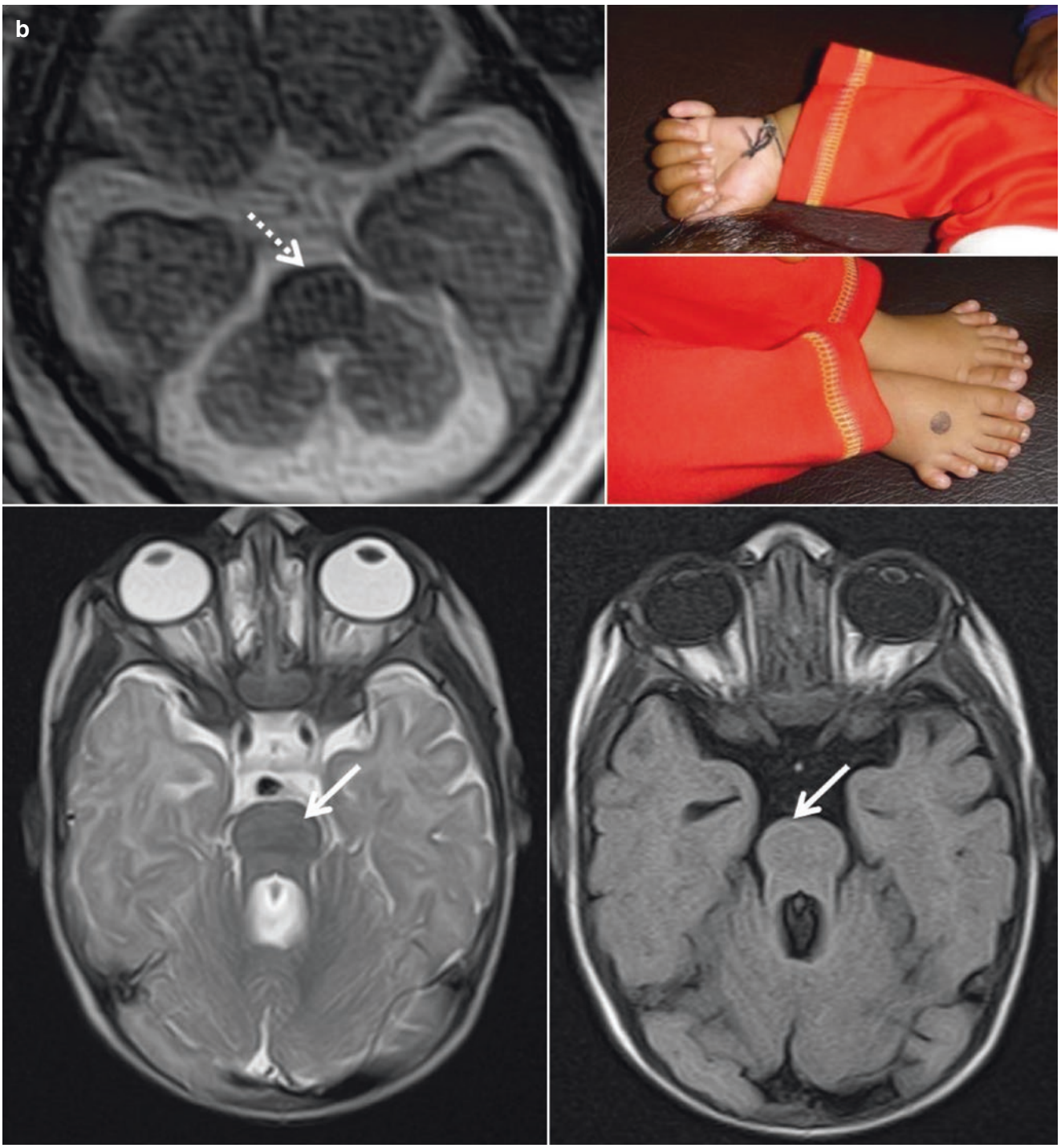

Fig. 5.21 (continued)

5. The above ultrasound features may not be seen in every case of Joubert syndrome. Hence absence of ultrasound or MRI findings does not rule out the condition.
6. In a few cases the vermian hypoplasia becomes apparent later in gestation.

As a screening modality in the general population, one should be alerted when there is an increased intracranial translucency in the 11–14 weeks scan or open fourth ventricle in the 18–23 weeks anomaly scan. These findings should be followed up by a detailed neurosonogram and fetal MRI if needed. When vermian hypoplasia is diagnosed, one must look for the 'molar tooth sign' on ultrasound and MRI. The differential diagnosis of an open fourth ventricle should be considered.

Joubert syndrome and the related disorders are caused by multiple gene mutations. Genetic counselling and molecular diagnosis may be offered.

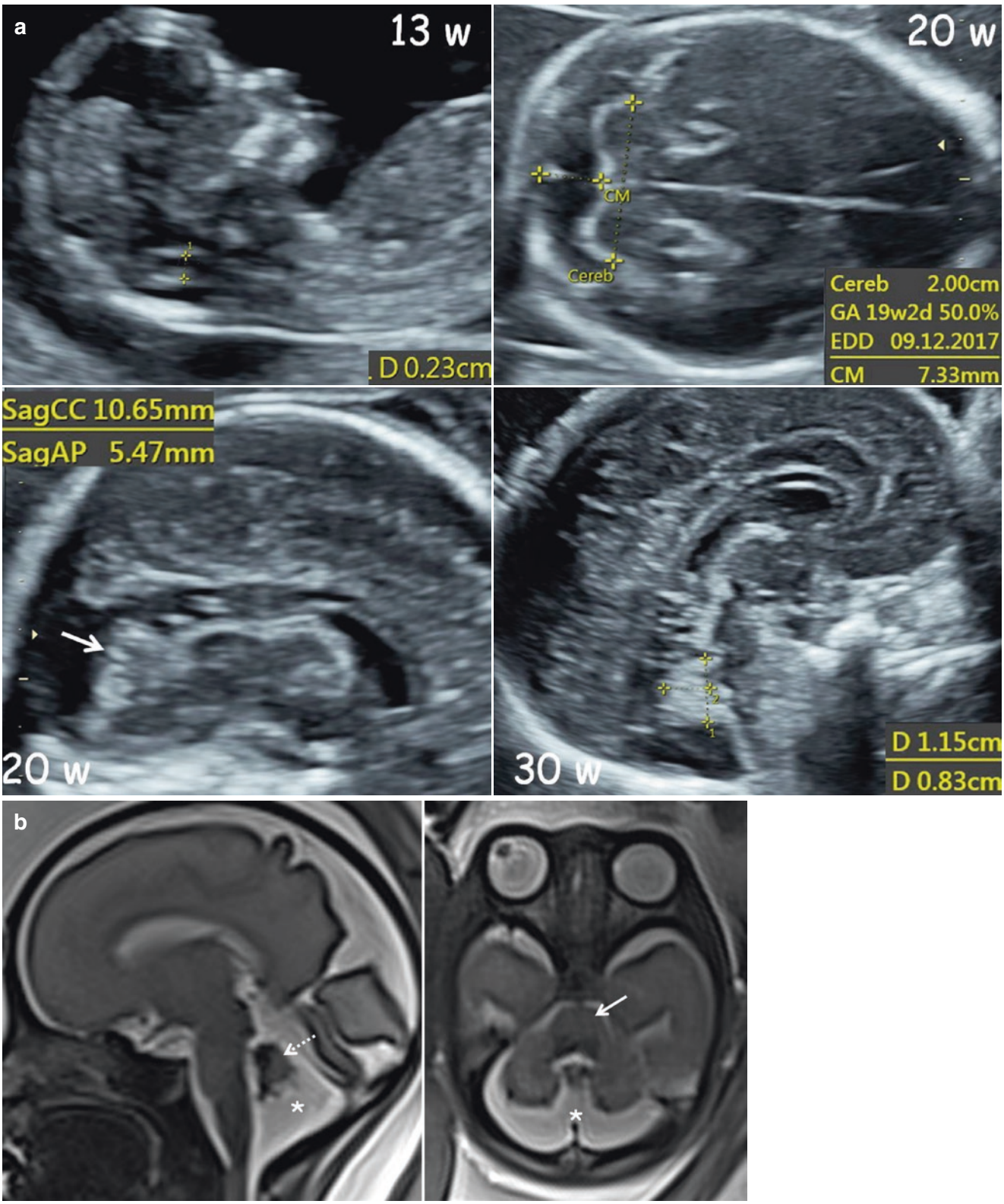

Fig. 5.22 (**a**) Third degree consanguineous couple with history of three previous postnatal deaths at 5–7 months of age. Two of them were reported as 'open fourth ventricle'; the last of them was diagnosed as *Joubert syndrome* (records of neurologist and geneticist). She is now in her fourth pregnancy. US studies were done at 13, 20 and 30 weeks (TAS and MRI). Midsagittal sections and axial transcerebellar section – normal intracranial translucency, normal TCD and AP depth of cisterna magna, normal vermian dimensions with no rotation (solid arrow) at 20 weeks, no vermian growth noted in the 30 weeks study confirming *vermian hypoplasia*, no vermian rotation noted, the cisterna magna is large consequent to the vermian hypoplasia. These findings indicate recurrence of Joubert syndrome. (**b**) Third-degree consanguineous couple with history of three previous postnatal deaths at 5–7 months of age. Two of them were reported as 'open fourth ventricle' on ultrasound; the last of them was a diagnosed as *Joubert syndrome* (neurology and geneticist's records) – 30 weeks (TAS and MRI) T2W midsagittal and transcerebellar axial sections – vermis is small but not rotated (dotted arrow), compensatory enlargement of cisterna magna (*), no evidence of 'molar tooth' sign (solid arrow). Vermian hypoplasia is indicative of *Joubert syndrome*

Suggested Reading

1. Katorza E, Bertucci E, Taschini S, Shanico K, Hoffmann C, Gilboa Y, Mazza V, Achiron R. Development of the fetal vermis: new biometry reference data and comparison of 3 diagnostic modalities-3D ultrasound, 2D ultrasound, and MR imaging. AJNR. 2016;37:1359–66.
2. Cignini P, Giorlandino M, Brutti P, Mangiafico L, Aloisi A, Giorlandino C. Reference charts for fetal cerebellar vermis height: a prospective cross-sectional study of 10605 fetuses. PLoS One. 2016;11(1):e0147528.
3. Zalel Y, Yagel S, Achiron R, Kivilevich Z, Gindes L. Three-dimensional ultrasonography of the fetal vermis at 18 to 26 weeks' gestation: time of appearance of the primary fissure. J Ultrasound Med. 2009;28:1–8.
4. Vinkesteijn AS, Mulder PG, Wladimiroff JW. Fetal transverse cerebellar diameter measurements in normal and reduced fetal growth. Ultrasound Obstet Gynecol. 2000;15:47–51.
5. Haratz KK, Shulevitz SL, Leibovitz Z, Lev D, Josef S, Tomarkin M, Malinger G, Lerman-Sagie T, Gindes L. The fourth ventricle index - a sonographic marker for severe fetal vermian dysgenesis/agenesis. Ultrasound Obstet Gynecol. 2018 [Epub ahead of print].
6. Massoud M, Cagneaux M, Garel C, Varene N, Moutard ML, Billette T, Benezit A, Rougeot C, Jouannic JM, Massardier J, Gaucherand P, Desportes V, Guibaud L. Prenatal unilateral cerebellar hypoplasia in a series of 26 cases: significance and implications for prenatal diagnosis. Ultrasound Obstet Gynecol. 2014;44:447–54.
7. Quarello E, Molho M, Garel C, Couture A, Legac MP, Moutard ML, Bault JP, Fallet-Bianco C, Guibaud L. Prenatal abnormal features of the fourth ventricle in Joubert syndrome and related disorders. Ultrasound Obstet Gynecol. 2014;43:227–32.
8. Pugash D, Oh T, Godwin K, Robinson AJ, Byrne A, Van Allen MI, Osiovich H. Sonographic 'molar tooth' sign in the diagnosis of Joubert syndrome. Ultrasound Obstet Gynecol. 2011;38:598–602.